



Occurrence and mobilization of radium in fresh to saline coastal groundwater inferred from geochemical and isotopic tracers (Sr, S, O, H, Ra, Rn)



David S. Vinson^{a,*}, Tarik Tagma^{b,1}, Lhoussaine Bouchaou^b, Gary S. Dwyer^a, Nathaniel R. Warner^{a,2}, Avner Vengosh^a

^a Duke University, Division of Earth & Ocean Sciences, Durham, NC, USA

^b Université Ibn Zohr, Faculté des Sciences, Laboratoire de Géologie Appliquée et Géo-Environnement, Agadir, Morocco

ARTICLE INFO

Article history:

Received 1 February 2013

Accepted 4 September 2013

Available online 13 September 2013

Editorial handling by M. Kersten

ABSTRACT

Salinization in groundwater systems can induce water–rock interaction, including the release of naturally-occurring trace elements of health significance such as radium (Ra), with possible implications for the usability of water resources in addition to the increase of dissolved solids (TDS) concentrations. In general, radium mobility is limited by chemical removal mechanisms including adsorption onto clays and/or Mn and Fe oxides, exchange processes, and coprecipitation with secondary barite. In order to examine the effect of aquifer salinity gradients on the distribution of naturally-occurring Ra in fresh to saline groundwater and the relationship to water–rock interaction and Ra removal mechanisms, two contrasting systems were investigated: the shallow unconfined coastal aquifer in Agadir (southwestern Morocco) and the confined Cretaceous (Cape Fear) and Pliocene (Yorktown) aquifers of the Atlantic Coastal Plain (North Carolina, USA). Geochemical and isotopic indicators of salinity sources (e.g. cation ratios, $\delta^{18}\text{O}$, $\delta^2\text{H}$, Br^-/Cl^- , $\delta^{34}\text{S}-\text{SO}_4^{2-}$, $\delta^{18}\text{O}-\text{SO}_4^{2-}$) were used to identify the relative contributions of seawater and other saline waters and subsequent geochemical modification by water–rock interaction. Radium activities (^{224}Ra , ^{226}Ra , ^{228}Ra), radon-222, alkaline earth metal (Mg, Ca, Sr, Ba) concentrations and ratios, and $^{87}\text{Sr}/^{86}\text{Sr}$ ratios were analyzed to identify water–rock interaction processes affecting alkaline earth metals including Ra. The Morocco coastal aquifer is generally oxic, exhibits a range of salinity and water types (Cl^- 163–2120 mg/L, median 932 mg/L), and exhibits Ca/Na ratios above the seawater value, typical of monovalent–divalent cation exchange (base-exchange reactions) in coastal aquifers. In contrast, the Atlantic Coastal Plain aquifers are anoxic, sulfate-reducing, cover a wider salinity range (Cl^- 5–9890 mg/L, median 800 mg/L) representing a transition between $\text{Na}-\text{HCO}_3^-$ and $\text{Na}-\text{Cl}^-$ waters, and exhibit Ca/Na ratios below that of modern seawater typical of reverse base-exchange reactions. Possible salinity sources in the Morocco coastal aquifer include seawater intrusion, Mesozoic evaporites, other natural saline waters, and/or wastewater, whereas the Atlantic Coastal Plain is primarily affected by old seawater present in the aquifer system. Radium activities are generally low and vary significantly within each aquifer, for example ^{226}Ra ranges from 1.8–27.7 mBq/L in the Morocco coastal aquifer (median 8.1 mBq/L) and 1.9–214 mBq/L in the Atlantic Coastal Plain (median 18.9 mBq/L). The highest Ra activities were observed in the most saline wells sampled in the Atlantic Coastal Plain. At total dissolved solids (TDS) concentrations above an apparent threshold of ~5000 mg/L, radium activities increase in a generally linear fashion with salinity in the Atlantic Coastal Plain, broadly comparable to previous studies indicating a threshold range of ~3000–10,000 mg/L. At lower TDS concentrations, water–rock interaction processes that vary with local aquifer conditions appear to control Ra distribution rather than merely salinity. In the Morocco coastal aquifer, adsorption of Ra and coprecipitation with secondary barite are apparently favorable to control Ra levels in groundwater. Radium removal in the anoxic Atlantic Coastal Plain aquifers appears to be associated with adsorption and/or exchange processes, with the additional possibility of barite precipitation in the Cape Fear aquifer indicated by barite saturation. Overall, the locally-variable factors that can control Ra sources and mobility in fresh to brackish groundwater at near-neutral pH include variation in solid-phase radioactivity, redox state affecting adsorption sites, availability of competing divalent cations, and barite saturation.

© 2013 Elsevier Ltd. All rights reserved.

* Corresponding author. Current address: Northwestern University, Department of Civil & Environmental Engineering, Evanston, IL, USA. Tel.: +1 847 491 3257; fax +1 847 491 4011.

E-mail address: david.vinson@northwestern.edu (D.S. Vinson).

¹ Current address: Hassan 1st University of Settat, Polydisciplinary Faculty of Khouribga, Hay Ezzaitouna, Khouribga 25000, Morocco.

² Current address: Department of Earth Sciences, Dartmouth College, Hanover, NH USA.

1. Introduction

Salinization of groundwater resources is a globally significant phenomenon; in many cases salinization occurs as a result of high groundwater demand where saline groundwater is present at depth or where salinity intrudes from adjacent surface water bodies (e.g. coastal aquifers), and may be exacerbated by drought and sea level rise. Heavily-exploited coastal aquifers may be impacted by a mixture of seawater, other natural saline waters and brines, agricultural effluents, and high-nitrate wastewater, as has been documented along the Atlantic coast of the United States (Barlow and Reichard, 2010; Vinson et al., 2011), northern Africa, and the Mediterranean region (Vengosh et al., 1999, 2002, 2005; Fakir et al., 2002; Bouchaou et al., 2008; de Montety et al., 2008; Ben Hamouda et al., 2011; Khaska et al., in press). In addition to the increase of total dissolved solids, which can require additional treatment or lead to the abandonment of wells, salinization can induce water–rock interaction including increased levels of naturally-occurring trace elements of health significance, such as radium (Ra), and further impair water quality. Modern seawater intrusion can in many cases be diagnosed and distinguished from other salinity sources using a combination of ion ratios and environmental isotopes including Br^-/Cl^- , Na/Cl^- , Ca/Na , Mg/Ca , $\delta^2\text{H}$, $\delta^{18}\text{O}$, and $\delta^{34}\text{S}$, and during salinization of complex aquifers, such as confined or highly developed coastal aquifers, delineating salinity sources may require a multi-tracer approach (Jones et al., 1999; Vengosh et al., 1999, 2002, 2005; Vengosh, in press). In such settings, the actual mechanisms governing the response of radium mobility to salinity gradients are not well understood (Swarzenski et al., 2013). A more detailed understanding of the Ra-salinity relationship would consider factors such as other interacting ions introduced by water–rock interaction, redox-sensitive Ra removal mechanisms, and estimation of salinity thresholds at which radium behavior is not approximated by the simple dilution of saline waters.

The objective of this study is to identify the occurrence and response of radium isotopes during the transition from fresh to saline groundwater. We have systematically examined the relative importance of the dissolved constituents that contribute to salinity and influence radium, including anion-driven effects associated with chloride and/or sulfate concentrations and effects associated with divalent cations. These factors are considered with respect to other potential influences on Ra, such as redox state. This study focuses on two contrasting aquifers in coastal regions (Fig. 1a): (1) the oxic coastal aquifer in the city of Agadir, Morocco that represents a typical unconfined coastal aquifer under conditions of salinization; and (2) the Atlantic Coastal Plain in North Carolina (USA), a confined, anoxic aquifer system containing saline water at depth and salinity increases in the shallower fresh aquifers in heavily-pumped areas. Through evaluation of the changing salinity and associated chemical evolution in these two different coastal zones, we aim to evaluate the role of the different factors on Ra distribution and occurrence in the salinized water.

A second objective of this investigation is to test and demonstrate the use of complementary isotope systems for understanding Ra sources and its removal mechanisms in fresh to brackish groundwater. The geochemical and isotopic tracers utilized in this study include ion ratios (e.g. Br^-/Cl^- , Na/Cl^- , Ca/Na), $\delta^2\text{H}$, $\delta^{18}\text{O}$, multi-isotopic radium analysis (^{224}Ra , ^{226}Ra , ^{228}Ra), radon-222, $^{87}\text{Sr}/^{86}\text{Sr}$ ratios, $\delta^{34}\text{S}$ of sulfate ($\delta^{34}\text{S}-\text{SO}_4^{2-}$), and $\delta^{18}\text{O}$ of sulfate ($\delta^{18}\text{O}-\text{SO}_4^{2-}$). Ion ratios, $\delta^2\text{H}$, and $\delta^{18}\text{O}$ were used to distinguish seawater from other sources of salinity (Jones et al., 1999; Vengosh et al., 2002, 2005; Vengosh, in press). Strontium isotopes were used to identify sources of divalent cations such as cation exchange (e.g. Katz and Bullen, 1996; Vengosh et al., 2002), information that can

be useful in tracing the mobility of divalent cations including radium. Sulfur and oxygen isotopes of sulfate were utilized to evaluate the sources of sulfate and sulfate reduction processes (Krouse and Mayer, 1999; Tuttle et al., 2009). Indirectly, isotopes of the sulfate ion were also used to assess the stability of the secondary mineral barite (BaSO_4), which removes radium by coprecipitation. The identification of sulfate-reducing conditions using isotopes of sulfate can provide information on the expected stability of barite. Altogether, the multi-isotope approach conducted in the two contrasting aquifers in this study, described below, provides better diagnostic tools to elucidate the origin and modification of radium isotopes during salinization conditions.

1.1. Unconfined urban coastal aquifer of Agadir, Morocco (MCA)

In the aquifer in and near the city of Agadir in western Morocco (Fig. 1b), transgressive marine aquifer sediments (limestone, sandstone, coquina, and marl) range from mid-Pliocene to early Pleistocene in age. In most of the study area, the ~100 m thick older Pliocene (Plaisancian–Astian) deposits are deeper than the typical depth of water wells. However, the lower portion of the Pliocene deposits outcrops in a structurally complex area near well M9-41, at the northern edge of the study area (Fig. 1b). The primary aquifer for most of the area is the overlying, Pliocene to Pleistocene (Villafranchian) transgressive deposits. This unit is composed of up to 100 m of marine clay, sand, gravel, and limestone, overlain by a wedge-shaped unit composed of conglomerate, sandy limestone, and shelly sandstone, with the sandstone and conglomerate being especially important water-yielding units. To the east (inland) these deposits are of fluvial–lacustrine origin (Dijon, 1969). Well depths, where known (Table 1), correspond mostly to the Villafranchian aquifer, which is interpreted as an unconfined aquifer. Typical of many heavily-exploited urban coastal aquifers in the Mediterranean region, elevated salinity and nitrate concentrations have been observed in the Agadir region (Hsissou et al., 2002; Bouchaou et al., 2008).

1.2. The Atlantic Coastal Plain (ACP) aquifer system, North Carolina, USA

The second groundwater system in this study is two confined aquifers in the coastal plain of North Carolina (eastern USA): the upper Cretaceous Cape Fear formation and the Pliocene Yorktown formation (Fig. 1c). The Cape Fear formation is interpreted as deltaic deposits including offshore components (Gohn, 1988; Winner and Coble, 1996), and contains a regional confining unit such that distinct upper and lower Cape Fear aquifers are defined in North Carolina. Although lithologically similar to the Upper Cape Fear aquifer, the lower Cape Fear aquifer exhibits higher salinity throughout most of its extent in North Carolina (Winner and Coble, 1996). The upper and lower Cape Fear aquifers are referred to together as the Cape Fear aquifer in this paper. The Yorktown aquifer is composed of marine sand and clay containing abundant shell material (Winner and Coble, 1996), and is locally phosphatic in the lower part of the formation (Riggs and Belknap, 1988). Both aquifers are of large subsurface extent and become thicker and more saline down-gradient towards the Atlantic Ocean, reaching salinity levels that would require treatment for use. In the areas sampled, the combined upper and lower Cape Fear aquifers are approximately 100 m thick, and the Yorktown aquifer is at least 100 m thick (Winner and Coble, 1996).

In North Carolina, the Coastal Plain aquifers are utilized for public water supply and industrial use. Water levels in wells have been declining for decades in heavily pumped areas (dePaul et al., 2008) and this is specifically the case in the wells sampled for this study, where declines of up to 10 m have been observed since 1980

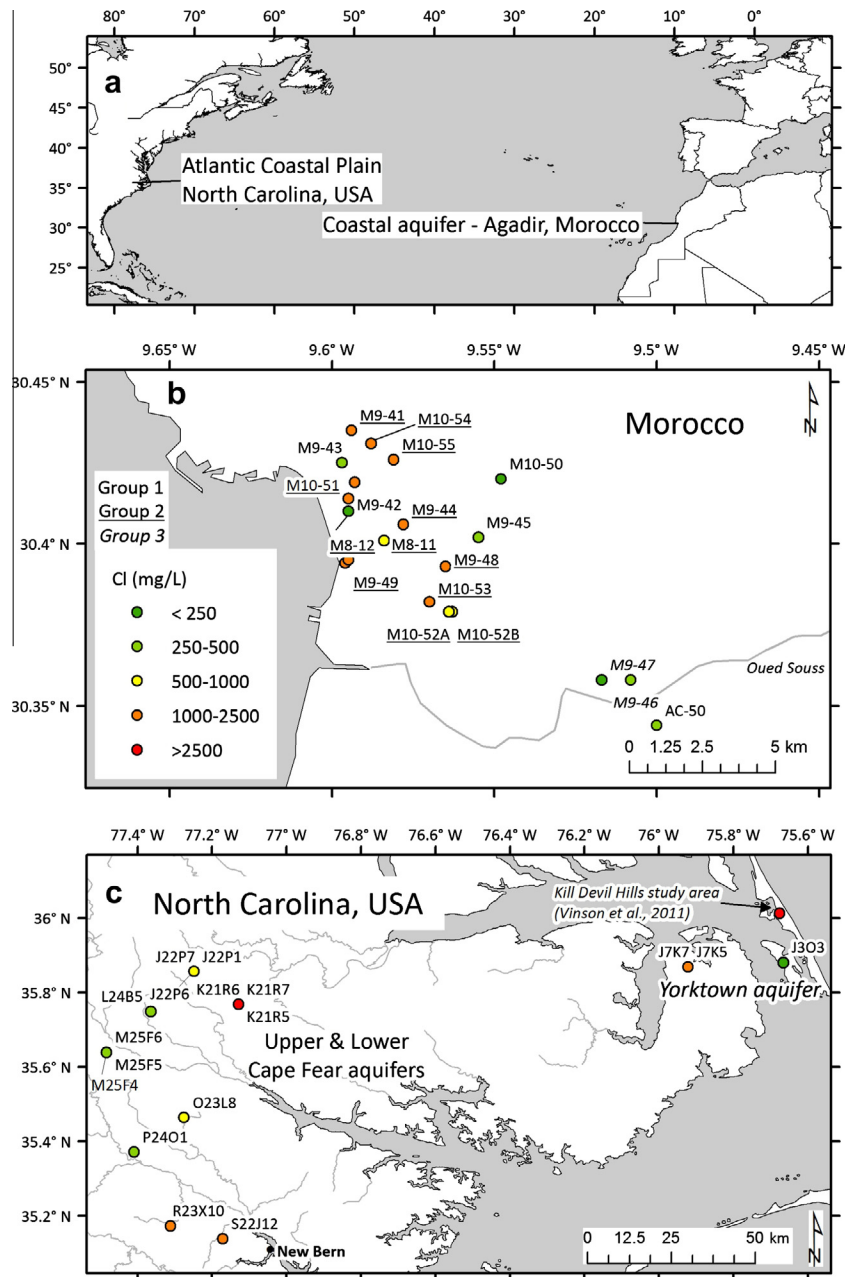


Fig. 1. Maps showing locations of study areas and wells sampled. In (c), Cl⁻ concentrations at multi-well sites (Table 1) are from the deepest and most saline well. Base map obtained from ArcGIS Online (panels a and b) and <http://www.nationalatlas.gov> (panel c).

(North Carolina Division of Water Resources data at <http://www.ncwater.org>). Deep saline water has leaked into freshwater wells in response to high pumping rates, and declining water levels in wells are associated with increasing chloride concentration (e.g. Vinson et al., 2011).

2. Methods

2.1. Sample collection

In order to examine a range of conditions, wells were selected along known salinity gradients in the Morocco coastal aquifer (Bouchaou et al., 2008; Tagma, 2005) and the Atlantic Coastal aquifers in North Carolina (North Carolina Division of Water Resources data at <http://www.ncwater.org>; Vinson et al., 2011). In the Morocco coastal aquifer, water samples were collected from

20 producing wells as close to the wellhead as possible and while pumps were operating. However, in some cases it was only possible to collect water samples after storage tanks. Atlantic Coastal Plain samples from the Cape Fear aquifer (14 wells) plus Yorktown aquifer samples J303, J7K5, and J7K7 were collected from wells in the monitoring network of the North Carolina Division of Water Resources. Monitoring wells were sampled after pumping three well water volumes, except wells M25F6, 1-510, and 1-610, which were sampled after approximately one volume. pH and dissolved oxygen concentration were measured at each sampling site on a minimally aerated flowing sample using meters that were calibrated daily. Samples from four Cape Fear wells, M25F4, M25F6, J22P7, and O23L8, contained notably high concentrations of suspended particles resulting in rapid clogging during filtration using 0.45 μm syringe-tip filters. Additional Yorktown Aquifer samples (12 Yorktown wells total) were collected from wells in the community of Kill Devil Hills as described by Vinson

Table 1
Major element concentrations (in mg/L). Data in *italics* appeared in Vinson et al. (2011).

Well	Depth (m)	Date	T (°C)	pH	O ₂	Ca	Mg	Na	K	Cl ⁻	Br ⁻	NO ₃ ⁻ as NO ₃ ⁻	SO ₄ ²⁻	HCO ₃ ⁻
<i>Morocco coastal aquifer (MCA)</i>														
<i>Group 1</i>														
AC-50		11 Mar 2008	24.3	6.9	1.7	125	107	123	7.8	257	0.5	90.3	139	
M9-42		19 May 2009	22.2	7.4	8.2	101	47.9	126	5.1	242	0.6	9.5	155	232
M9-43		19 May 2009	25.1	7.2	5.6	127	103	160	6.2	396	1.4	0.4	149	465
M9-45		19 May 2009	25.3	6.8	5.9	179	112	225	6.2	398	1.0	13.2	358	474
M10-50	130	18 Mar 2010	26.1	7.5		87.2	48.7	96.5	4.4	163	0.5	0.1	63.2	468
<i>Group 2</i>														
AC-43		11 Mar 2008	24.4	6.8	4.1	230	183	1050	9.3	1860	5.8	37.2	482	
M8-11		18 Dec 2008	24.0	7.0	3.4	191	148	411	6.7	843	2.7	8.6	370	408
M8-12		18 Dec 2008	23.4	7.1	3.9	243	201	663	13.5	1530	4.8	27.6	444	413
M9-41	70	19 May 2009	24.0	6.8	6.5	259	138	376	6.7	1020	3.4	55.7	166	474
M9-44		19 May 2009	24.8	6.9	7.2	400	291	627	11.9	1870	6.2	43.2	605	402
M9-48		27 May 2009	24.8	6.9	4.2	254	165	418	7.2	1160	3.9	15.1	332	351
M9-49	80	29 May 2009	23.1	7.0	0.2	251	207	687	16.1	1480	4.6	28.9	423	457
M10-51	70	18 Mar 2010	23.9	7.1		236	192	966	9.8	1880	6.4	59.5	555	585
M10-52A		18 Mar 2010	24.2	7.0		169	111	428	5.4	703	2.0	45.3	450	560
M10-52B		18 Mar 2010	22.8	7.1		182	117	412	6.2	739	2.1	33.3	483	534
M10-53		18 Mar 2010	23.6	7.0		363	230	777	9.1	2120	7.1	20.9	500	455
M10-54		18 Mar 2010	25.6	6.9		341	192	478	5.8	1680	5.5	45.8	188	370
M10-55	90	18 Mar 2010	25.3	7.1		280	167	511	6.8	1440	4.7	71.0	262	357
<i>Group 3</i>														
M9-46		20 May 2009	23.3	6.9	0.5	242	195	235	6.0	433	0.6	25.2	816	490
M9-47	61	20 May 2009	23.7	7.2	4.1	165	112	155	3.8	236	0.5	1.2	522	481
<i>Atlantic Coastal Plain (ACP) – Yorktown aquifer</i>														
J303	67	10 Dec 2008	17.5	7.2	0.3	49.5	4.2	67.0	4.9	49.8	0.2		0.2	265
J7K7	27	11 Dec 2008	17.8	6.8		54.0	23.0	27.7	18.8	22.1	0.1		0.4	356
J7K5	96	11 Dec 2008	18.5	7.9	0.3	17.9	29.7	1080	42.4	1340	4.9		64.2	586
Ocean Bay	~120	28 Oct 2008		8.6	0.3	4.6	6.0	511	4.5	336	1.3		27.2	717
Albatross	~120	28 Oct 2008	18.8	8.0	0.3	20.6	42.7	950	3.7	1150	4.1		21.5	515
1-310	95	28 Oct 2008		8.0	0.7	4.8	6.1	469	1.5	357	1.3		24.2	574
Production well 1	~90–120	28 Oct 2008	20.0	7.9	0.6	63.2	112	1570	82.9	2400	8.7		168	354
1-510	156	28 Oct 2008	21.4	7.2	0.2	232	479	4990	168	8180	29.6		764	333
1-610	187	28 Oct 2008	21.4	7.2	0.1	270	527	5820	207	9890	36.4		719	458
Production well 2	~90–120	28 Oct 2008	20.0	7.8	1.6	72.2	128	1650	88.0	2520	9.1		191	371
Production well 7	~90–120	28 Oct 2008	19.5	7.8	0.6	79.1	128	1640	74.1	2610	9.3		177	313
Production well 11	~90–120	28 Oct 2008		7.8	0.7	66.5	122	1720	74.4	2740	10.1		187	410
<i>Atlantic Coastal Plain (ACP) – Upper and Lower Cape Fear aquifers</i>														
L24B5	119	18 Oct 2007	18.5	7.6		4.7	7.0	658	29.0	379	1.3		286	334
M25F4	86	19 Oct 2007	19.5	7.8		5.5	2.0	80.9	9.3	8.8	<0.1		7.7	204
M25F5	101	19 Oct 2007	19.1	8.1	0.4	1.3	0.9	133	10.6	62.3	0.2		26.1	213
M25F6	173	19 Oct 2007	21.8	8.1		12.4	11.1	928	31.9	457	1.6		304	725
J22P6	187	22 Oct 2007	20.4	8.0	0.3	17.1	20.2	1100	39.4	774	2.7		459	729
J22P7	157	22 Oct 2007	20.0	7.7	0.2	5.6	6.3	530	24.8	402	1.5		232	567
J22P1	90	22 Oct 2007	18.7	7.3	0.3	18.9	18.4	60.0	22.5	4.6			0.4	302
K21R5	286	22 Oct 2007	22.4	7.4	0.2	95.0	132	3550	114	4680	16.6		1090	531
K21R6	226	10 Dec 2008	20.8	7.5	0.4	53.9	81.7	2720	85.1	3040	10.8		1140	633
K21R7	133	10 Dec 2008	19.1	8.5	0.3	3.9	1.4	258	12.7	79.7	0.3		58.0	467
P2401	216	11 Dec 2008	20.7	7.6	0.2	4.8	3.6	647	18.3	369	1.4		317	622
R23X10	307	13 Jan 2009	22.5	7.6	0.8	25.6	20.9	1810	47.7	2450	10.9		305	390
S22J12	323	13 Jan 2009	22.0	7.2	0.4	19.2	14.0	1600	45.5	2040	8.9		115	647
O23L8	256	13 Jan 2009	20.5	7.7	0.8	8.9	8.0	926	26.2	825	3.2		252	762
Seawater (Millero and Sohn, 1991)				8.2		412	1280	10800	399	19400	67		2710	114

et al. (2011). These include a site consisting of a monitoring well (1-310), production well (well 1), and two deeper monitoring wells (1-510 and 1-610; Table 1).

2.2. Major and trace elements

Sodium, Ca, Mg, Fe, and Mn concentrations were determined on filtered samples (0.45 µm) by direct current plasma (DCP) spectrometry, and K was analyzed by flame atomic absorption spectrometry, both calibrated using standards prepared from plasma-grade single-element standards. Barium and Sr concentrations were determined by inductively-coupled plasma mass spectrometry, calibrated using NIST 1643e trace element solution. Major anions (Cl⁻, NO₃⁻, SO₄²⁻, Br⁻) were analyzed on filtered samples by ion

chromatography, and alkalinity was determined by titration of unfiltered water samples to pH 4.5. Barium saturation index values were calculated using the PHREEQC geochemical code, version 2 (Parkhurst and Appelo, 1999).

2.3. Stable isotopes ($\delta^2\text{H}$, $\delta^{18}\text{O}$, $\delta^{34}\text{S}-\text{SO}_4^{2-}$, $\delta^{18}\text{O}-\text{SO}_4^{2-}$)

Hydrogen and oxygen isotopes of water samples were analyzed at the Duke University Environmental Isotope Laboratory with a ThermoFinnigan thermochemical analyzer and Delta+XL isotope ratio mass spectrometer on the peaks of H₂ and CO gas, normalized to the VSMOW and VSLAP standards and reported as $\delta^2\text{H}$ and $\delta^{18}\text{O}$ with precision of 0.3‰ and 0.1‰, respectively. Sulfur and oxygen isotope ratios of sulfate ($\delta^{34}\text{S}-\text{SO}_4^{2-}$, $\delta^{18}\text{O}-\text{SO}_4^{2-}$) were analyzed

from BaSO₄ precipitates which were prepared by extracting ~7 mg of sulfate from filtered water samples using BaCl₂ and filtering the resulting precipitate onto glass fiber filters at Duke University. The sulfate was analyzed at the University of Calgary Isotope Science Laboratory. Sulfur isotope ratios were analyzed by continuous flow isotope ratio mass spectrometry, normalized to VCDT using NIST and IAEA sulfate standards, and reported as δ³⁴S–SO₄²⁻ with precision of 0.25‰. Oxygen isotopes of sulfate were analyzed by reacting BaSO₄ in a thermochemical analyzer and determining the δ¹⁸O of the resulting CO gas using a Delta+XL mass spectrometer. As a check on the purity of BaSO₄ precipitate, δ¹⁸O–SO₄²⁻ data are reported only from samples containing 27 ± 2% oxygen. These ratios were normalized to VSMOW, also using NIST and IAEA sulfate standards, and reported as δ¹⁸O–SO₄²⁻ with precision of 0.3‰.

2.4. Strontium, radium, and radon isotopes

Samples were prepared and analyzed for strontium isotope ratios at Duke University on a ThermoFisher TRITON thermal ionization mass spectrometer. To prepare samples, ~3 μg Sr was dried in a Teflon vial on a hot plate in a laminar flow hood, redissolved in Optima HNO₃, separated with Eichrom SR-B50-S resin (procedural blank <80 pg Sr), and loaded onto degassed Re filaments in a Ta loading solution. The 1σ analytical error is 0.000010 based on long-term replicate analysis of the NIST 987 standard.

For radium analysis, unfiltered water samples were collected in polyethylene containers and processed later the same day. Most samples were 50–52 L, but a few samples were of different volume (26–78 L). Samples were slowly pumped through sequential columns (typically two), each containing 10 g (dry weight) of commercially-obtained Mn oxide-impregnated acrylic fibers, then rinsed and squeezed of excess water. Manganese oxide fibers from each extraction column were analyzed separately for ²²⁴Ra using a delayed coincidence counter (Moore and Arnold, 1996; Garcia-Solsona et al., 2008) at an efficiency for hand-squeezed fibers. Radium-224 activities were decay-corrected to the time of collection. Radium-226 was sealed in a glass tube and analyzed after a 21-day incubation period with a DurrIDGE RAD7 radon-in-air monitor (Kim et al., 2001), calibrated with NIST 4969 and 4967 ²²⁶Ra solutions that had been transferred onto Mn oxide fibers. Radium-228 of the upper column's fibers was analyzed in a compressed disc geometry (65 mm diameter × 5 mm thick) on a Canberra germanium gamma detector using the 911 keV peak of ²²⁸Ac, calibrated with two equilibrated ²³²Th (²²⁸Ra) rock and one compressed Mn fiber standards loaded in matching geometry. The sample-specific detection limit, 1.96σ, is defined by Eaton et al. (2005) as the activity with 95% probability of being detected at ±100% precision. The stated uncertainties of radium isotope results are based on counting statistics only (Eaton et al., 2005; Garcia-Solsona et al., 2008), which include the propagation of error (Eaton et al., 2005) associated with background subtraction and addition of activities from the individual columns. The counting errors do not incorporate other potential uncertainties including moisture content (²²⁴Ra) or counting geometry (²²⁸Ra) variation. A limited number of samples were collected from Cape Fear aquifer wells for radon-222 analysis in glass vials without headspace and sent overnight to a commercial laboratory for analysis by liquid scintillation counting.

3. Comparison of salinity characteristics

3.1. Observed salinity trends in the investigated aquifers

In the Morocco coastal aquifer, ion concentrations vary across approximately a factor of ten within the study area (Na 96–1050 mg/L; Cl⁻ 242–2120 mg/L; SO₄²⁻ 63–816 mg/L; Table 1). The

spatial distribution of salinity is irregular. Although the highest-chloride waters occur, in general, closest to the Atlantic Ocean, there is no systematic trend in salinity with distance from the coast (Fig. 1c). Waters in this aquifer are generally oxalic (Table 1), although dissolved oxygen concentrations are maximum values due to the possibility of aeration prior to sampling of some wells. Using element concentrations, distinctive ion ratios, and diagnostic isotope signatures, three groups of waters were identified: (1) relatively fresh (TDS < 1800 mg/L) waters in which bicarbonate exceeds 25% of anions (as equivalents; samples M9-42, M9-43, M9-45, AC-50, and M10-50); (2) Cl-dominated waters (51–81% of anions) with SO₄²⁻/Cl⁻ < 0.25, δ³⁴S–SO₄²⁻ of 13.0–17.3‰, and TDS > 2000 mg/L; and (3) a distinctive high-sulfate (43–45% of anions), low-chloride water exhibiting SO₄²⁻/Cl⁻ > 0.5, δ³⁴S–SO₄²⁻ ≤ -8.0‰, and TDS > 1000 mg/L, located near the Oued Souss (samples M9-46 and M9-47; Fig. 1; Tables 1 and 2). Cation composition overlaps significantly between these three salinity groups. Although the most Na-dominated waters are located near the Atlantic Ocean, ion ratios exhibit deviations from expected seawater values, even in group 2 waters where seawater influence appears most evident: (1) SO₄²⁻/Cl⁻ is above the seawater value of 0.05 (group 2 median 0.11, range 0.04–0.24); (2) Na/Cl⁻ is below the seawater value of 0.86 (group 2 median 0.69, range 0.44–0.87; Fig. 2a); and (3) Ca/Na is above the seawater value of 0.02 (group 2 range 0.13–0.41; Fig. 2b). Br⁻/Cl⁻ ratios were observed throughout MCA near and slightly below the expected seawater value of 1.5 × 10⁻³.

Within the Atlantic Coastal Plain (ACP) aquifers, dissolved solids concentrations gradually increase down-gradient and in areas associated with high groundwater pumping in the aquifers, encompassing a larger range and reaching higher salinity than in the Morocco coastal aquifer (Na 28–5820 mg/L, Cl⁻ 5–9890 mg/L, SO₄²⁻ < 1–1140 mg/L). Several changes in the major cation composition were observed down-gradient in the ACP aquifers: increasing cation dominance by Na, increasing Cl⁻ concentrations, and generally increasing sulfate concentrations (Table 1). Sodium is nearly uniformly the dominant cation (median 92% Na + K as equivalents, range 27–98%). Higher sodium dominance was observed in the Cape Fear aquifer (median 96% Na + K) than in the Yorktown aquifer (median 84% Na + K). Consistent patterns were also observed in divalent cations. In both ACP aquifers, Mg is significantly lower than the expected Mg/Cl⁻ ratio from seawater (Fig. 2c). In the Yorktown aquifer, Ca/Cl⁻ and Sr/Cl⁻ are at or above seawater values; in the Cape Fear aquifer, Ca/Cl⁻ and Sr/Cl⁻ are at or below seawater values (Fig. 2d and e). Br⁻/Cl⁻ ratios are uniformly close to the seawater value of 1.5 × 10⁻³.

3.2. Discussion of salinity sources and water–rock interaction in the coastal aquifers

3.2.1. Salinity sources and salinization mechanisms

In MCA, the fresh end member (approximated by group 1 waters) exhibits a Ca–Mg–HCO₃⁻ composition characteristic of initial equilibration of fresh recharge with carbonate-rich aquifer solids, consistent with previously published δ¹³C and carbon-14 activities (Bouchaou et al., 2008). Fresh, Ca–Mg–HCO₃⁻ waters at or near calcite saturation are subsequently modified by saline inputs. Evidence that the coastal aquifer receives a combination of salinity sources, possibly including modern seawater, wastewater, and Mesozoic (Atlas Mountains) evaporites (Hsissou et al., 2002; Bouchaou et al., 2008) includes: (1) saline waters found several km inland (Fig. 1); (2) varied nitrate concentrations (median 27.6 mg/L as NO₃⁻, range 0.1–90.3 mg/L); and (3) values of Br⁻/Cl⁻ below the seawater value (6.0–8.7 × 10⁻⁴) in the low-Cl⁻, high-SO₄²⁻/Cl⁻ waters of group 3. As with major element concentrations, δ¹⁸O and δ²H do not record systematic seawater inputs to the coastal aquifer. Instead, δ¹⁸O and δ²H are consistent with the global meteoric water line and with

Table 2
Trace metal concentrations and isotope ratios. Data in *italics* appeared in [Vinson et al. \(2011\)](#).

Well	TDS ^a (mg/L)	$\delta^2\text{H}$ (‰)	$\delta^{18}\text{O}$ (‰)	$\delta^{34}\text{S}-\text{SO}_4^{2-}$ (‰)	$\delta^{18}\text{O}-\text{SO}_4^{2-}$ (‰)	Fe (mg/L)	Sr (mg/L)	$^{87}\text{Sr}/^{86}\text{Sr}$	Ba ($\mu\text{g/L}$)	^{224}Ra (mBq/L)	^{226}Ra (mBq/L)	^{228}Ra (mBq/L)	^{222}Rn (Bq/L)
<i>Morocco coastal aquifer</i>													
<i>Group 1</i>													
AC-50				16.7	8.5	0.05	1.04	0.709622	52.8	12.4 ± 1.3	9.8 ± 1.5	4.9 ± 2.2	
M9-42	919	-22.2	-3.5	11.6	10.4	0.02	0.89	0.708676	61.5	5.1 ± 0.4	3.9 ± 0.7	5.8 ± 2.1	
M9-43	1407	-16.0	-3.4	-2.2	11.6	0.03	1.67	0.708469	62.6	16.7 ± 1.3	25.5 ± 1.6	35.8 ± 8.8	
M9-45	1765	-30.6	-4.9	16.0		0.05	2.10	0.708348	23.0	6.4 ± 0.6	2.8 ± 0.6	8.8 ± 2.8	
M10-50	930	-25.9	-5.5				0.93	0.708684	80.4	18.1 ± 1.2	27.7 ± 1.5	20.1 ± 4.7	
<i>Group 2</i>													
AC-43				15.2	6.1	0.37	2.81	0.708691	41.4	19.9 ± 1.3	4.2 ± 1.2	6.9 ± 1.8	
M8-11	2386					0.01	2.39	0.708484	32.6	24.0 ± 1.7	8.5 ± 1.1	12.6 ± 3.6	
M8-12	3530					0.03	4.42	0.708770	74.9	26.8 ± 1.8	8.2 ± 0.9	20.9 ± 5.0	
M9-41	2500	-19.3	-3.2	13.0	6.5	0.04	1.73	0.708671	102	25.3 ± 1.8	20.4 ± 2.1	18.2 ± 5.1	
M9-44	4249	-29.0	-4.8	16.4	9.1	0.04	5.78	0.708524	45.5	34.5 ± 2.4	7.7 ± 0.9	34.8 ± 8.4	
M9-48	2700	-38.9	-5.9	17.3		0.37	2.95	0.708396	45.9	23.6 ± 1.6	5.8 ± 1.0	13.4 ± 3.8	
M9-49	3550	-31.6	-4.9	17.3	9.2	0.35	4.08	0.708727	69.2	32.4 ± 2.1	8.0 ± 1.0	18.5 ± 5.0	
M10-51	4483	-24.5	-3.9			0.14	3.09	0.708652	31.6	14.8 ± 1.1	6.3 ± 0.9	9.0 ± 2.5	
M10-52A	2472	-40.6	-6.5			0.02	2.00	0.708576	21.4	17.2 ± 1.3	5.0 ± 1.0	9.6 ± 2.5	
M10-52B	2506	-33.5	-5.1			0.02	2.14	0.708579	22.3				
M10-53	4470	-35.7	-5.6			0.04	4.84	0.708602	48.7	34.2 ± 2.3	10.6 ± 1.0	16.4 ± 3.9	
M10-54	3300	-20.9	-3.8			0.04	2.13	0.708865	145	41.2 ± 2.6	17.3 ± 1.3	32.8 ± 6.8	
M10-55	3100	-26.5	-4.2			0.20	2.23	0.708726	105	30.5 ± 2.3	17.0 ± 1.3	35.9 ± 7.6	
<i>Group 3</i>													
M9-46	2442	-27.8	-4.5	-8.0		0.03	2.10	0.709516	37.1	6.5 ± 0.5	1.8 ± 0.6	6.0 ± 2.2	
M9-47	1676	-34.3	-6.0	-9.1	2.8		1.53	0.709287	39.4	8.2 ± 0.5	3.6 ± 0.6	12.1 ± 3.1	
<i>Atlantic Coastal Plain (ACP) – Yorktown aquifer</i>													
J303	441	-21.8	-4.3			0.81	0.27	0.709058	8.6	4.8 ± 0.7	3.3 ± 0.7	6.0 ± 3.2	
J7K7	502	-20.5	-4.6			3.80	0.37	0.709156	15.9	6.4 ± 0.9	5.6 ± 0.8	4.6 ± 2.6	
J7K5	3150	-16.4	-3.7			0.29	0.70	0.708997	6.9	7.0 ± 0.9	4.6 ± 1.7	2.8 ± 2.0	
Ocean Bay	1610	-20.1	-4.1			0.09	0.10	0.709148	4.0	1.7 ± 0.4	2.5 ± 0.5	<0.9	
Albatross	2700	-20.7	-4.3				0.90	0.709052	2.4	4.9 ± 0.8	4.9 ± 0.7	3.8 ± 1.3	
1-310	1440					0.07	0.09	0.709000	1.3	1.9 ± 0.5	1.9 ± 0.6	<1.2	
Production well 1	4750			34.4	21.1	0.55	2.83	0.709052	8.0	21.4 ± 0.9	19.1 ± 1.3	19.5 ± 3.4	
1-510	15150	-10.8	-2.3	34.7	21.8	2.65	13.8	0.709028	50.9	99.1 ± 7.3	186 ± 7	96.7 ± 21.7	
1-610	17890	-9.7	-2.2	36.5	22.4	2.59	18.0	0.709028	67.2	98.7 ± 6.1	214 ± 7	119 ± 26	
Production well 2	5020					0.68	2.97	0.709040	8.8	19.1 ± 1.0	20.0 ± 1.3	24.0 ± 4.6	
Production well 7	5020	-18.7	-3.4			0.70	3.45	0.709038	10.9	25.6 ± 1.7	26.9 ± 1.5	27.0 ± 6.3	
Production well 11	5320	-16.7	-3.5			0.65	3.44	0.709027	9.3	29.2 ± 2.4	26.9 ± 1.7	26.3 ± 6.8	
<i>Atlantic Coastal Plain (ACP) – Upper and Lower Cape Fear aquifers</i>													
L24B5	1697					0.12	0.05	0.708709	16.3	23.5 ± 1.6	9.4 ± 1.2	15.4 ± 4.4	8.5
M25F4	318					0.02	0.02	0.708683	25.3	29.8 ± 1.8	21.5 ± 1.4	30.8 ± 9.1	3.3
M25F5	447					0.10	0.01	0.708877	28.7	3.6 ± 0.7	4.4 ± 0.9	<2.9	15.1
M25F6	2469					0.30	0.08	0.708881	58.7	39.8 ± 2.9	28.0 ± 1.9	55.1 ± 15.9	28.5
J22P6	3041			29.4	20.7	0.05	0.17	0.708506	29.8	18.4 ± 1.2	10.6 ± 1.3	17.9 ± 4.9	52.1
J22P7	1767					0.07	0.06	0.708641	28.1	23.6 ± 1.9	39.5 ± 2.1	11.5 ± 6.0	2.9
J22P1	427					0.25	0.19	0.708945	704	42.7 ± 2.0	18.6 ± 1.4	51.4 ± 14.1	3.3
K21R5	10190					0.62	2.06	0.709065	27.7	257 ± 14	105 ± 5	175 ± 30	8.8
K21R6	7750			29.0		0.55	1.19	0.708922	20.6	74.9 ± 3.4	32.0 ± 1.4	60.8 ± 5.6	
K21R7	881					0.10	0.03	0.708673	41.5	8.1 ± 1.0	4.3 ± 0.6	5.7 ± 1.3	
P24O1	1982			31.2	21.1	0.17	0.06	0.708943	25.5	6.2 ± 0.8	14.1 ± 1.2	6.2 ± 1.5	
R23X10	5050					0.15	0.78	0.708127	31.8	28.4 ± 2.2	26.5 ± 2.0	18.5 ± 2.3	
S22J12	4480			30.6	20.1	0.16	0.82	0.708084	58.7	66.1 ± 3.2	30.0 ± 1.9	53.9 ± 4.7	
O23L8	2808					0.29	0.17	0.708994	39.1	17.1 ± 1.1	14.8 ± 1.3	12.6 ± 2.0	
Seawater	35100			21.0 ^b	9.5 ^b		7.9 ^c	0.70924 ^b	14 ^c				

^a TDS reported as sum of major ions in [Table 1](#).

^b [Clark and Fritz \(1997\)](#).

^c [Millero and Sohn \(1991\)](#).

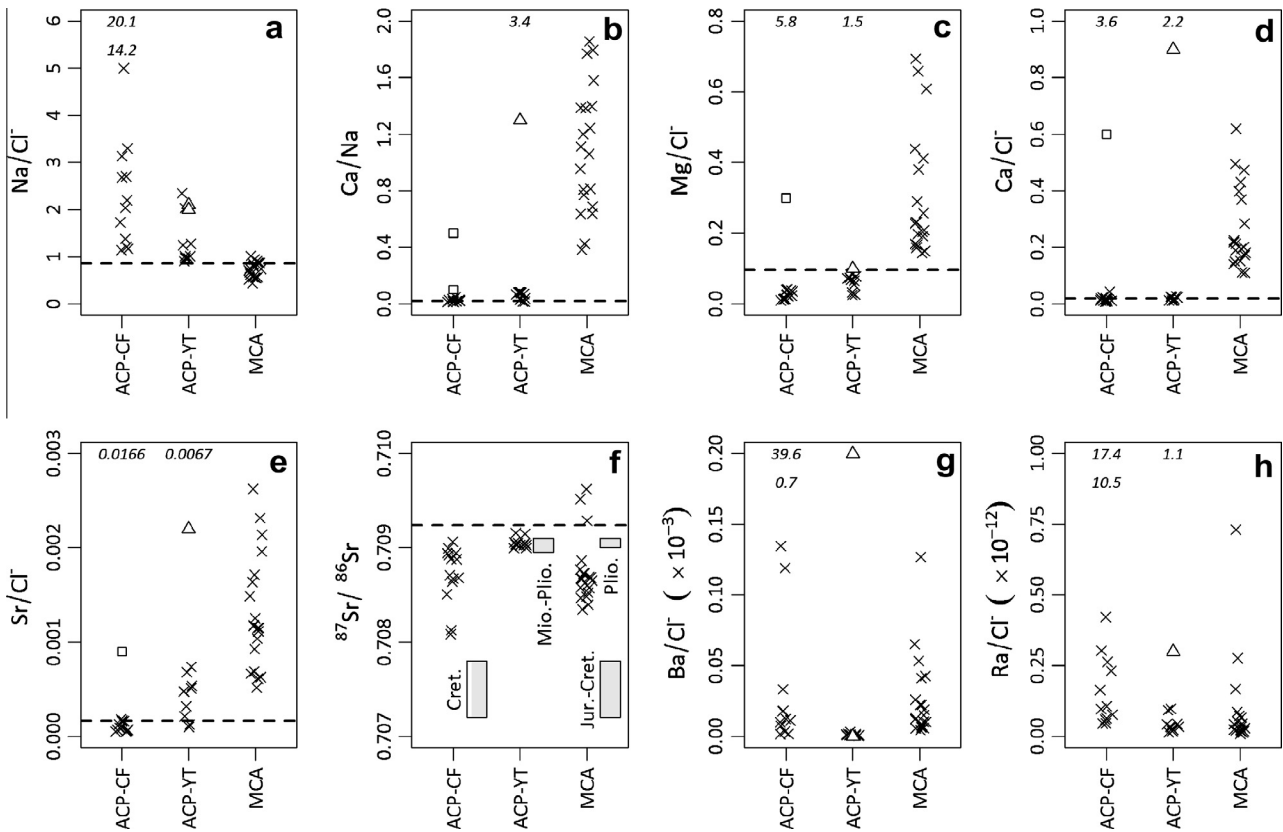


Fig. 2. Comparative ion (all in mol/mol) and strontium isotope ratios diagnostic of solute sources and cation exchange in the Atlantic Coastal Plain (ACP) and Morocco coastal aquifer (MCA). Dashed lines indicate modern seawater values of each ratio. Values for shallow ACP wells (Section 3.2.1) are represented by squares (Cape Fear aquifer – CF), triangles (Yorktown aquifer – YT), and numbers indicating off-scale values. Shaded bands represent $^{87}\text{Sr}/^{86}\text{Sr}$ values of marine carbonates of indicated ages (McArthur et al., 2001).

Atlantic-derived Moroccan precipitation (Ouda et al., 2005). In MCA, salinity cannot be described in terms of a single seawater intrusion front, but is instead contributed by multiple salinity sources, as is typical of heavily-exploited urban coastal aquifers. The geographic areas of high chloride (group 2) and sulfate concentrations (group 3) have been identified previously (Dijon, 1969; Hsissou et al., 2002; Tagma, 2005; Bouchaou et al., 2008); therefore, salinity increases are probably gradual in the MCA.

In contrast to MCA with its multiple natural and anthropogenic sources of salinity, the association between $\delta^2\text{H}$, $\delta^{18}\text{O}$, and chloride concentration in the Atlantic Coastal Plain aquifers consistently indicates a seawater-derived salinity source (Vinson et al., 2011). However, the seawater-like salinity in the ACP aquifers is not modern seawater intrusion, but instead represents old, modified and diluted seawater from previous sea level fluctuations (Meisler, 1989). The shallowest ACP wells (J7K7, J3O3, M25F4, and J22P1) are also the least Na-dominated (26–56% Na + K). These wells exhibit higher Mg/Cl^- , Ca/Cl^- , and Sr/Cl^- ratios than the deeper, more Na-dominated waters (Fig. 2).

Major element composition of the ACP aquifers is consistent with the vertical and down-gradient trends described in previous investigations, in which a distinctive combination of ion exchange and mixing phenomena is observed: (1) Recharging waters interacted with carbonate material, yielding fresh Ca-Mg-HCO_3^- groundwater; (2) Farther down-gradient, reverse base-exchange reactions occurred in which divalent cations were removed and monovalent cations, primarily Na^+ , were released; (3) CO_2 from microbial respiration drove carbonate shell dissolution, with subsequent Ca removal by cation exchange, yielding increased TDS within the Na-HCO_3^- water type; and (4) Na-HCO_3^- waters mixed

with deep saline Na-Cl^- waters that represent modified seawater from prior sea level fluctuations (Chapelle and Knobel, 1983, 1985; Chapelle et al., 1987; Meisler, 1989; McMahon and Chapelle, 1991; Knobel et al., 1998). The natural freshening process yielding Na-HCO_3^- waters (step 2 above) represents the progressive reversal of old seawater intrusion through fresh groundwater recharge to the Atlantic Coastal Plain aquifers. The long residence time of fresh to brackish groundwater in confined ACP aquifers ($>10^4$ -years; e.g. Kennedy and Genereux, 2007) indicates that progressive freshening along the ~ 200 km-long aquifer in North Carolina is slow, whereas large variations in chloride concentration can occur on human time scales in response to pumping.

3.2.2. Divalent cation release and $^{87}\text{Sr}/^{86}\text{Sr}$

In MCA, strontium isotope ratios fall within a narrow range (0.70835–0.70887; Fig. 2f) for all but three samples in the southeastern part of the study area (0.70929–0.70962; Fig. 3), representing group 3 plus sample AC-50 and exhibiting more radiogenic values than the other samples and also higher than modern seawater (Table 2). In ACP, $^{87}\text{Sr}/^{86}\text{Sr}$ differs substantially between the Cape Fear and Yorktown aquifers. In the Yorktown aquifer, $^{87}\text{Sr}/^{86}\text{Sr}$ falls within a narrow range (0.70898–0.70916, median 0.70904), but ratios occupy a larger range in the Cape Fear aquifer and are less radiogenic (0.70813–0.70895, median 0.70871; Fig. 2f). There is no apparent relationship between $^{87}\text{Sr}/^{86}\text{Sr}$ and Sr concentration in either ACP aquifer, nor was this expected given the systematic removal of divalent cations.

A distinctive phenomenon during seawater intrusion is Ca/Na exchange, resulting in Ca enrichment in the salinized groundwater relative to seawater abundance (Nadler et al., 1980; Jones et al.,

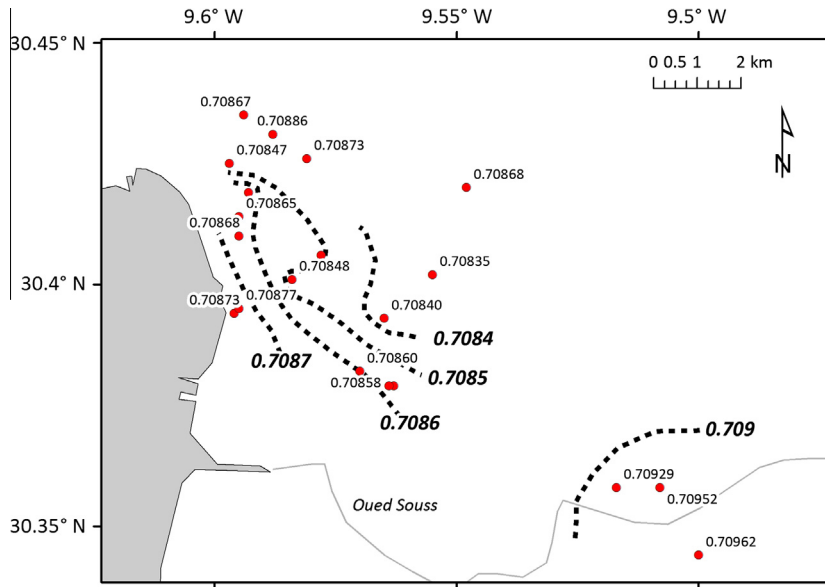


Fig. 3. Map showing distribution of $^{87}\text{Sr}/^{86}\text{Sr}$ ratios within the Morocco coastal aquifer, with contours of inferred geographic trends. Base map obtained from ArcGIS Online.

1999; Vengosh et al., 2002; Sivan et al., 2005; Russak and Sivan, 2010). Apparent cation exchange is here indicated by ΔNa that represents the difference of cation concentrations relative to seawater diluted to the same chloride concentration as the groundwater. Assuming seawater to be the chloride source, ΔNa is consistent with release or uptake of cations from exchange sites (e.g. Vengosh et al., 2002; Russak and Sivan, 2010):

$$\Delta\text{Na} = [\text{Na}] - [\text{Cl}] \left(\frac{[\text{Na}]_{\text{sw}}}{[\text{Cl}]_{\text{sw}}} \right) \quad (1)$$

in which $[\text{Na}]$, $[\text{Cl}]$, $[\text{Na}]_{\text{sw}}$, $[\text{Cl}]_{\text{sw}}$ are the sodium and chloride concentrations (in meq/L) of groundwater and seawater, respectively. In MCA, ΔNa plotted against ΔCa is close to the line of slope -1 (Fig. 4) consistent with Ca/Na exchange, but slightly higher in divalent cations than can be accounted for by cation exchange alone. The probable source of additional Ca is dissolution of carbonate minerals, and the effect of excess Ca is most apparent at samples with $\Delta\text{Na} < 10$ meq/L, that is, those least affected by salinization (Fig. 4), consistent with the Ca–Mg– HCO_3^- composition of the fresh end member.

In MCA, high Sr/Cl $^-$ ratios (Fig. 2e) indicate widespread release of Sr from aquifer solids. Because of the systematic release of divalent cations, including Sr, during seawater intrusion, $^{87}\text{Sr}/^{86}\text{Sr}$ can

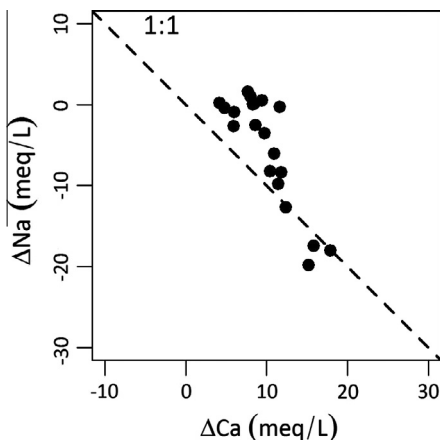


Fig. 4. ΔNa vs. ΔCa as an indicator of cation exchange in the Morocco coastal aquifer. The line of slope -1 is consistent with Ca–Na ion exchange (Section 3.2.2).

record the signatures of seawater and/or salinization-induced water–rock interaction (e.g. Vengosh et al., 2002; Bouchaou et al., 2008). $^{87}\text{Sr}/^{86}\text{Sr}$ is especially diagnostic in coastal aquifers because $^{87}\text{Sr}/^{86}\text{Sr}$ of seawater Sr has varied systematically over geologic time, in particular increasing continuously for ~ 40 million years (Eocene/Oligocene to present; McArthur et al., 2001), allowing marine, nonmarine, and anthropogenic cation sources to be distinguished in many cases. Observed values of $^{87}\text{Sr}/^{86}\text{Sr}$ are both above and below the modern seawater ratio, but most waters exhibit less radiogenic values, indicating additions of older marine-derived strontium (Table 2). The majority of $^{87}\text{Sr}/^{86}\text{Sr}$ values are also less radiogenic than the inferred Pliocene age of the aquifer sediments (0.7090–0.7091) but significantly more radiogenic than the Mesozoic marine sedimentary rocks of the western Atlas Mountains (0.7082–0.7083; McArthur et al., 2001). Also, in the waters exhibiting $^{87}\text{Sr}/^{86}\text{Sr} < 0.709$, ratios generally decrease inland (Fig. 3). This may indicate increasing seawater influence near the coastline and/or increasing inputs of less radiogenic Mesozoic Sr to the more inland wells. In any case, the observed $^{87}\text{Sr}/^{86}\text{Sr}$ ratios are inconsistent with a mixture of Sr from modern seawater and the Pliocene aquifer solids alone. $^{87}\text{Sr}/^{86}\text{Sr}$ is consistent with Sr release to the aquifer from marine-derived solids of pre-Pliocene age but does not confirm presence of modern seawater in the aquifer. The three samples with $^{87}\text{Sr}/^{86}\text{Sr} > 0.709$ are located along the Oued Souss and more inland than the other sampling sites (Fig. 3). These values apparently represent nonmarine Sr sources.

In much of the ACP aquifer system and in contrast to MCA, exchange sites remain Na-saturated from interaction of marine clays with seawater as reverse base-exchange releases Na into groundwater while removing Ca to the solids during gradual freshening (Chapelle and Knobel, 1983). Therefore, the relationship between cation composition and salinity is the opposite of apparent patterns in MCA. Furthermore, most waters in the ACP are dominated by Na, higher than the seawater proportion (Fig. 2a). $^{87}\text{Sr}/^{86}\text{Sr}$ is not associated with salinity in the ACP aquifers, nor should any correlation be expected because the aquifer undergoes mixing of Na– HCO_3^- and Na–Cl $^-$ waters without divalent cation release being induced by this mixing. Values of $^{87}\text{Sr}/^{86}\text{Sr}$ are uniformly lower than the modern seawater ratio and primarily reflect prolonged water–rock interaction with the different aquifer rocks. The ratios observed in Cape Fear aquifer groundwater (0.70808–0.70906), being more

radiogenic than Cretaceous seawater (Fig. 2f), are probably influenced by continental-source Sr such as mica (Brown, 1959) and feldspar (Gohn, 1988) present in the formation. In the Yorktown aquifer, $^{87}\text{Sr}/^{86}\text{Sr}$ falls within a narrow range (0.70900–0.70916) that corresponds with late Miocene to late Pliocene marine carbonates (Fig. 2f). These results are consistent with studies from the North Carolina coastal plain indicating agreement with the global seawater $^{87}\text{Sr}/^{86}\text{Sr}$ record in Tertiary carbonate-bearing formations (Denison et al., 1993) and groundwater in these formations (Woods et al., 2000).

4. Specific components of salinity and redox conditions: Effects on radium behavior

4.1. Overview of Ra isotope geochemistry in aquifers

4.1.1. Steady-state Ra sources and removal mechanisms

Four naturally-occurring radioactive isotopes of radium occur from the alpha decay of thorium isotopes in the ^{238}U , ^{232}Th , and ^{235}U decay series, of which ^{224}Ra , ^{226}Ra , and ^{228}Ra , with half-lives ranging from 3.6 days to 1600 years, are addressed in this investigation. As described by Krishnaswami et al. (1982), the expected steady-state balance (groundwater Ra activity not changing) of Ra source and removal mechanisms in groundwater can be represented by:

$$P + k_2 C_s = \lambda C + k_1 C \quad (2)$$

in which P is the nuclide's supply rate, k_2 is the first-order rate constant of desorption, C_s is desorbable solid-phase radium in atoms per unit of water, C is the atomic concentration of a radium isotope in water, λ is the nuclide's decay constant, and k_1 is the first-order rate constant of adsorption. Recoil occurs during the alpha decay of the parent thorium isotopes on the aquifer solids, releasing radium into water. In the case of radium isotopes, P mostly represents the alpha recoil flux; only ^{226}Ra is sufficiently long-lived (half-life = 1600 yr) that minor weathering input is possible (Krishnaswami et al., 1982).

At steady state, recoil plus desorption are balanced by *in situ* radioactive decay plus chemical removal to the solids. In fresh, oxic groundwater at near-neutral pH, $P \gg k_2 C_s$ because desorption is relatively inefficient under these conditions; and $\lambda C \ll k_1 C$, because $\lambda \ll k_1$ for radium isotopes in contact with rock surfaces (Krishnaswami et al., 1982, 1991; Swarzenski et al., 2013). Because Ra in groundwater is derived from local water–rock interaction, solid-phase availability of parent nuclides is a major control on P and therefore also on groundwater Ra levels. However, a recent review of Ra occurrence in the United States noted that some of the highest-Ra groundwater occurred in formations inferred to have among the lowest solid-phase radioactivity (Szabo et al., 2012). Therefore, P alone does not predict Ra in groundwater, but instead, at steady state, $P \approx k_1 C$; that is, recoil is balanced primarily by variable chemical removal mechanisms controlled by water chemistry.

The main mechanisms of chemical Ra removal include charge-sensitive removal (adsorption/cation exchange) and coprecipitation into barite (BaSO_4). Especially in fresh, oxic groundwater at near-neutral pH, radium is adsorbed rapidly on the aquifer solids. Effective Ra adsorption sites include Mn and Fe oxides, principally Mn oxides with their negative surface charge at near-neutral pH (Moore and Reid, 1973; Ames et al., 1983b); and clays and zeolites (Nathwani and Phillips, 1979; Ames et al., 1983a). Cation exchange is distinguished from adsorption in that cation exchange is more reversible than adsorption, involving outer-sphere surface complexes and the diffuse-ion swarm, rather than inner-sphere surface complexes characteristic of specific adsorption (Sposito, 2008). As adsorption and cation exchange are linked to the cation's charge

and the surface charge of aquifer solids among other factors, they were not distinguishable by the methods of this field-based investigation.

Another potentially significant mechanism is the coprecipitation of Ra in solid solution with its chemical analogue Ba in the secondary mineral barite (BaSO_4). The rate of Ba sulfate precipitation in actual groundwater systems is not well constrained, and it has been inferred that where exchange sites are abundant, exchange processes dominate radium removal rather than coprecipitation (Shao et al., 2009). Overall, calculated values of k_1 imply that Ra isotopes are generally removed within minutes in fresh groundwater (Krishnaswami et al., 1982). The possible competition between charge-sensitive removal (cation exchange or desorption) vs. coprecipitation was also addressed by Szabo et al. (2012), who noted that in sulfate-dominated waters ^{226}Ra is negatively correlated with sulfate concentration, implying that coprecipitation is significant in removing radium. Conversely, in bicarbonate-dominated waters, ^{226}Ra is positively correlated with sulfate, implying that sulfate plays the expected role of saline influxes by mobilizing radium (Szabo et al., 2012). Also supporting the potential importance of coprecipitation when not prevented by bacterial sulfate reduction, a positive relationship has been observed between ^{226}Ra in water and the occurrence of sulfate-reducing conditions (Martin et al., 2003). Furthermore, high Ra levels have been widely observed in BaSO_4 scale in oil fields (e.g. Zielinski and Budahn, 2007), and indeed, the highest reported Ra activities are in sulfate-free brines (Kraemer and Reid, 1984; Rowan et al., 2011; Warner et al., 2012; Haluszczak et al., 2013). Together, these observations suggest that sulfate can impart a radium-removing effect through BaSO_4 precipitation in diverse groundwater systems.

In addition to changes in Ra activity, Ra isotope ratios can provide useful information on Ra behavior. Radium isotope ratios are typically reported as the ratios of short-lived to long-lived activities ($^5\text{Ra}/^1\text{Ra}$), such as $^{228}\text{Ra}/^{226}\text{Ra}$ and $^{224}\text{Ra}/^{228}\text{Ra}$. $^5\text{Ra}/^1\text{Ra}$ can vary in groundwater systems because Ra is removed at a rate dependent on concentration without regard to half-life, whereas individual Ra isotopes are replenished by alpha recoil at rates that depend on their respective half-lives. The steady-state value of $^{228}\text{Ra}/^{226}\text{Ra}$ is approximately equal to the $^{232}\text{Th}/^{238}\text{U}$ activity ratio of the aquifer solids (Dickson, 1990). The steady-state value of $^{224}\text{Ra}/^{228}\text{Ra}$ is thought to be at or slightly above the secular equilibrium ratio of unity in groundwater systems (Krishnaswami et al., 1982; Tricca et al., 2001; Reynolds et al., 2003).

4.1.2. Radium response to environmental conditions

Numerous studies have documented a relationship between radium levels and salinity in saline groundwater at near-neutral pH (Kraemer and Reid, 1984; Miller and Sutcliffe, 1985; Krishnaswami et al., 1991; Moise et al., 2000; Sturchio et al., 2001; Tomita et al., 2010; Szabo et al., 2012; Swarzenski et al., 2013). With the rapid introduction of saline water, Ra release by desorption can become significant, while chemical removal of radium becomes relatively inefficient ($P + k_2 C_s > k_1 C$; Eq. (2)). Radium levels in water can rapidly increase under these non-steady-state conditions. Radium desorption has been documented from suspended sediments during mixing of fresh river water and seawater (Li and Chan, 1979; Webster et al., 1995; Krest et al., 1999) and during injection of brine into bedrock fractures (Wood et al., 2004). However, in aquifers with stable salinity, Ra input to groundwater typically occurs through alpha recoil from the abundant Th isotopes on the aquifer solids, while Ra retention is through chemical removal mechanisms such as adsorption onto clay minerals and oxides in the aquifer (Section 4.1.1). In aquifers in which salinity increases gradually, alpha recoil is probably more important as a Ra source than direct Ra desorption, and therefore a significant mechanism by which radium activity increases with salinity is that radium

removal subsequent to recoil becomes less efficient (that is, k_1 decreases). In estimations of k_1 and k_2 variations using the model of Krishnaswami et al. (1982), k_1 typically decreases by a factor of approximately 10^4 between fresh water and brines, whereas k_2 would typically increase by only a factor of approximately 10 across this range (Krishnaswami et al., 1982, 1991; Swarzenski et al., 2013). Mechanisms by which k_1 can decline systematically with increasing salinity, causing groundwater Ra to increase, include competition for adsorption and exchange sites with other divalent cations and/or complexation with anions, principally RaCl^+ and RaSO_4^0 , that prevents direct adsorption of Ra^{2+} .

As another example of effects specific to major ion composition, it has been documented that Ca and other divalent cations, where present at high concentrations, successfully compete with Ra for adsorption sites (Nathwani and Phillips, 1979; Szabo et al., 2012; Swarzenski et al., 2013). In addition, some important Ra adsorption sites in the subsurface are redox-sensitive (Mn and Fe oxides; Section 4.1.1), commonly yielding high Ra in fresh anoxic waters at near-neutral pH (Szabo and Zapezca, 1987; Szabo et al., 2012; Vinson et al., 2012). Furthermore, because many saline aquifers are also anoxic, and specifically seawater intrusion is often associated with sulfate-reducing conditions as high-sulfate waters contact organic-rich marine sediments (Appelo and Postma, 1993; Andersen et al., 2005; Sivan et al., 2005; Yamanaka and Kumagai, 2006; de Montety et al., 2008), the relative roles of salinity-sensitive mechanisms vs. redox conditions in inducing higher radium levels in saline groundwater (e.g. Herczeg et al., 1988) remain less well understood.

On some time scale, the response of Ra to changing environmental conditions is recorded by $^5\text{Ra}/^1\text{Ra}$ ratios (Section 4.1.1). The difference in decay constants between ^{228}Ra and ^{226}Ra (half-lives of 5.8 yr and 1600 yr respectively) implies that in response to a salinity increase, groundwater ^{228}Ra activity would increase via alpha recoil faster than ^{226}Ra , resulting in above-equilibrium $^{228}\text{Ra}/^{226}\text{Ra}$ ratios until steady state is reached. Examples of dynamic environments in which high $^{228}\text{Ra}/^{226}\text{Ra}$ (e.g., >4) is documented are beach and intertidal subsurface waters (Lamontagne et al., 2008; Michael et al., 2011; Otero et al., 2011). As with $^{228}\text{Ra}/^{226}\text{Ra}$, strong dominance of ^{224}Ra relative to ^{228}Ra has been observed in dynamic mixing settings (e.g. $^{224}\text{Ra}/^{228}\text{Ra} > 2$ in intertidal subsurface waters; Lamontagne et al., 2008; Michael et al., 2011). The spatial scale over which elevated $^5\text{Ra}/^1\text{Ra}$ ratios can occur is restricted. For example, Michael et al. (2011) estimated that saline, low-Ra water (e.g. seawater) would reach steady-state ^{226}Ra activity within 200 m of entering an aquifer; steady-state activities of shorter-lived Ra isotopes would be reached even more rapidly.

4.2. Results of radium and barium analysis

The highest-salinity groundwater samples, primarily observed in the Yorktown Aquifer but also to a lesser extent in the Cape Fear aquifer, are associated with the highest levels of radium in groundwater (up to 99 Bq/L ^{224}Ra , 214 Bq/L ^{226}Ra , and 119 Bq/L ^{228}Ra). Radium in groundwater only exhibits a clear positive linear association with chloride and TDS concentration in the most saline waters from the ACP aquifers (Fig. 5a and b). At salinity levels below ~ 2500 mg/L Cl^- (~ 5000 mg/L TDS), no systematic relationship between Ra and salinity is evident in the groundwater investigated during this study. Only in the Yorktown aquifer was a linear Ra-salinity relationship observed at TDS concentration as low as 3000 mg/L. The specific Ra-mobilizing conditions in each aquifer, discussed below, may explain the more complex Ra behavior observed in less saline waters.

In the Morocco coastal aquifer, radium isotope activities are generally correlated with each other (reported as Spearman rank coefficient ρ): ^{224}Ra and ^{228}Ra ($\rho = 0.71$), ^{228}Ra and ^{226}Ra ($\rho = 0.67$), and ^{224}Ra and ^{226}Ra ($\rho = 0.55$). The relationship between radium and salinity is more complex. Radium-224, the shortest-

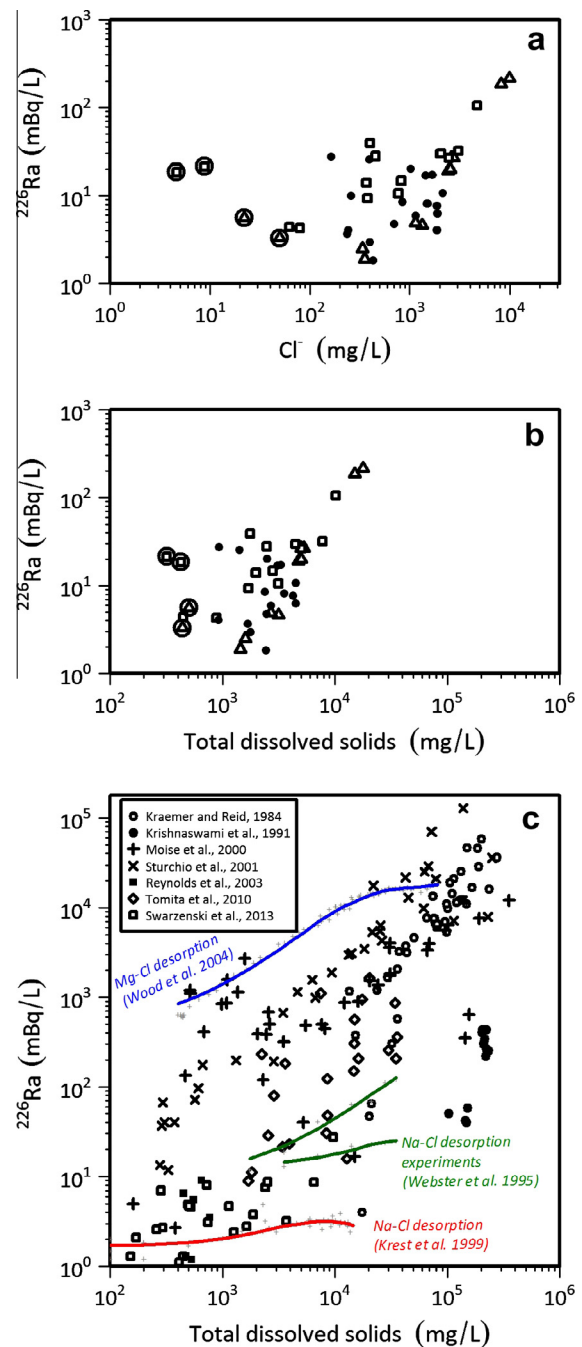


Fig. 5. Plots depicting ^{226}Ra activities from the studied aquifers in relation to chloride (a) and TDS concentrations (b). Circled data points represent the shallow ACP waters (Section 3.2.1). In panel (c), the ^{226}Ra -TDS relationship in groundwater (incorporating data presented and reviewed by Tomita et al. (2010)) is superimposed on desorption trends during freshwater-seawater mixing (Na- Cl^- waters; Webster et al., 1995; mixing samples of $<15\%$ salinity of Krest et al. (1999)) and injection of Mg- Cl^- brine into bedrock fractures (Wood et al., 2004). Note that direct Ra desorption alone may be responsible for approximately a factor of 5–30 radium increase in water without receiving α -recoil as a continuous source of Ra input. Desorption trends plotted using the LOWESS smoothing function (R Core Team, 2013).

lived Ra isotope, is positively correlated with TDS and major ion concentrations (Ca, Cl^- , Mg, Na, and K ($\rho \geq 0.50$)), but not with sulfate concentration ($\rho = 0.06$). In contrast, the longest-lived radium isotope ^{226}Ra is not well correlated with major ions ($\rho < 0.45$), except that it is somewhat negatively correlated with sulfate concentration ($\rho = -0.60$). Radium-228, of intermediate half-life, exhibits

correlation patterns between those of ^{224}Ra and ^{226}Ra . The correlations reported in this Section generally weaken when the high-sulfate, high- $^{87}\text{Sr}/^{86}\text{Sr}$ waters (group 3 and sample AC-50) are excluded from the analysis, which could imply that local geographic variability of aquifer solids, rather than groundwater chemistry, affects the prevalence of ^{228}Ra vs. ^{226}Ra . As with radium isotopes and salinity overall, barium concentrations vary within approximately a factor of ten (21–145 $\mu\text{g/L}$). Barium concentration is well correlated with ^{226}Ra activity ($\rho = 0.72$) and exhibits progressively weaker correlations with ^{228}Ra ($\rho = 0.61$) and ^{224}Ra ($\rho = 0.51$) activities. Barium's relationship to salinity is similar to that of ^{226}Ra , rather than the shorter-lived ^{224}Ra and ^{228}Ra .

In the ACP aquifers overall, the three radium isotopes in this study exhibit positive correlations with each other: ^{224}Ra and ^{228}Ra ($\rho = 0.96$), ^{228}Ra and ^{226}Ra ($\rho = 0.89$), and ^{224}Ra and ^{226}Ra ($\rho = 0.91$). Radium is also positively correlated with TDS concentration ($\rho = 0.57, 0.58, \text{ and } 0.69$ for $^{224}\text{Ra}, ^{228}\text{Ra}, \text{ and } ^{226}\text{Ra}$, respectively), and more strongly so in the Yorktown aquifer ($\rho = 0.90, 0.82, \text{ and } 0.86$ for $^{224}\text{Ra}, ^{228}\text{Ra}, \text{ and } ^{226}\text{Ra}$, respectively). In addition, as with salinity overall, radium is well-correlated with chloride and sulfate concentrations in the Yorktown aquifer (for sulfate, $\rho = 0.84, 0.74, \text{ and } 0.81$ for $^{224}\text{Ra}, ^{228}\text{Ra}, \text{ and } ^{226}\text{Ra}$, respectively), but much less so in the Cape Fear aquifer (for sulfate, $\rho = 0.22, 0.36, \text{ and } 0.34$ for $^{224}\text{Ra}, ^{228}\text{Ra}, \text{ and } ^{226}\text{Ra}$, respectively). The Cape Fear aquifer exhibits higher overall Ra/Cl^- ratios than the Yorktown aquifer (Fig. 2h), which may relate to differences in aquifer source material. In contrast to the overall correlation of radium with salinity in the ACP aquifers, the Cape Fear and Yorktown aquifers exhibit differences in the apparent relationship between Ra and Ba. In the Cape Fear aquifer, Ba concentration is essentially uncorrelated with Ra isotopes ($\rho = 0.05, 0.05, \text{ and } -0.04$ for $^{224}\text{Ra}, ^{228}\text{Ra}, \text{ and } ^{226}\text{Ra}$, respectively), whereas the Yorktown aquifer exhibits positive correlations between Ra and Ba ($\rho = 0.74, 0.84, \text{ and } 0.81$ for $^{224}\text{Ra}, ^{228}\text{Ra}, \text{ and } ^{226}\text{Ra}$, respectively). The observed levels of Ra, Ba, and other divalent cations can be separated into (1) the comparatively shallow waters containing more Ra and Ba relative to the Ra-salinity trend and therefore exhibiting higher Ba/Cl^- and Ra/Cl^- ratios (Fig. 2g and h); and (2) deeper waters along the transition from $\text{Na}-\text{HCO}_3^-$ to $\text{Na}-\text{Cl}^-$ water type in which divalent cations are systematically removed. Notably, the four shallowest ACP waters exhibit higher levels of Ra than might be expected by their chloride or TDS concentrations alone (circled points in Fig. 5a and b). This might be connected to their substantially higher Ca/Na ratios than the deeper ACP waters (Fig. 2b), indicating more competition for Ra removal sites by other alkaline earth metals than in the more Na-dominated waters. In the deeper, down-gradient portions of the ACP aquifers, radium activities increase with salinity (Fig. 5), primarily evident at higher chloride concentrations than were observed in MCA.

4.3. Discussion of radium mobility and relationship to environmental conditions

Broadly, the observed radium-salinity trends in this study are consistent with some previous studies of brackish-saline groundwater in that a linear Ra-salinity trend is seen primarily above TDS concentrations of ~ 3000 – $10,000$ mg/L (Fig. 5b and c). Of the previous studies shown in Fig. 5c, only Sturchio et al. (2001) documented a consistent linear radium-salinity relationship at $\text{TDS} < 1000$ mg/L in a carbonate aquifer in the midwestern USA. The large overall salinity difference between fresh and saline groundwater can be compared to environments in which rapid salinity increases cause direct Ra desorption from sediments, in which Ra increases steeply with increased salinity before leveling off as desorption appears complete. Observed salinity levels at which desorption is apparently complete are $\sim 10,000$ mg/L in

coastal zone surface waters (Krest et al., 1999), $\sim 20,000$ – $30,000$ mg/L in experimental sediment-seawater mixing (Webster et al., 1995), and $\sim 30,000$ mg/L during desorption of Ra from bedrock fractures by $\text{Mg}-\text{Cl}^-$ brine (Wood et al., 2004; Fig. 5c). Radium in groundwater exhibits larger increases across a large salinity range than implied by trends during direct Ra desorption from sediments (Fig. 5c). This points to the role of alpha recoil as a continual input of Ra in aquifers that is removed with decreasing efficiency as salinity increases, in addition to the direct Ra desorption that occurs. Finally, all pH measurements in this study are near-neutral (Table 1), minimizing the need to consider the significant effects on radium expected in acidic waters. It should be emphasized that the near-neutral pH groundwater investigated during this study exhibits distinct Ra behavior from the low-TDS, acidic groundwater in the shallow aquifers at the upper edge of the Atlantic Coastal Plain, where excessive Ra levels have been documented (e.g. Szabo et al., 1997, 2012; Bolton, 2000).

4.3.1. Radium isotope ratios

In the Morocco coastal aquifer (Section 4.2), sulfate concentrations are somewhat correlated with $^{228}\text{Ra}/^{226}\text{Ra}$ ($\rho = 0.65$ or 0.46 if the three high- $^{87}\text{Sr}/^{86}\text{Sr}$ points are excluded), but not with chloride ($\rho = 0.19$ or 0.32 if the high- $^{87}\text{Sr}/^{86}\text{Sr}$ points are excluded). It should be noted that high sulfate concentration and $^{228}\text{Ra}/^{226}\text{Ra}$ are somewhat associated with lower ^{226}Ra activity (possible removal of Ra). This is inconsistent with non-steady-state salinization in which elevated $^{228}\text{Ra}/^{226}\text{Ra}$ corresponds to increased radium in groundwater (Section 4.1.2) and implies that $^{228}\text{Ra}/^{226}\text{Ra}$ may record variation of the solid-phase Th/U ratio in MCA.

Within the ACP aquifers, $^{228}\text{Ra}/^{226}\text{Ra}$ averaging < 1 in the Yorktown aquifer (median 0.9) is consistent with its marine carbonate content, as carbonate systems have a higher affinity for U than Th (Moise et al., 2000; Sturchio et al., 2001; Szabo et al., 2012; Vinson et al., 2012). In the Cape Fear aquifer, $^{228}\text{Ra}/^{226}\text{Ra}$ generally ≥ 1 (median 1.6) is consistent with sandstone aquifers containing Ra from nonmarine sources (e.g. Vengosh et al., 2009; Szabo et al., 2012). Given that $^{87}\text{Sr}/^{86}\text{Sr}$ in the ACP aquifer system seems to record marine carbonate vs. nonmarine detrital sources of Sr (Section 3.2.2), $^{228}\text{Ra}/^{226}\text{Ra}$ ratios averaging ≥ 1 (continental sandstone) and < 1 (marine carbonate) are consistent with steady-state lithologic controls on the observed $^{228}\text{Ra}/^{226}\text{Ra}$, rather than $^{228}\text{Ra}/^{226}\text{Ra}$ representing non-steady-state Ra mobilization (Section 4.2).

Median $^{224}\text{Ra}/^{228}\text{Ra}$ values of the waters throughout this study were near or slightly above 1 (median 1.3 in MCA, 1.2 in Cape Fear, 1.1 in Yorktown). Therefore as with $^{228}\text{Ra}/^{226}\text{Ra}$ indicating mainly lithologic control, $^{224}\text{Ra}/^{228}\text{Ra}$ is consistent with alpha recoil as the primary radium source balanced by chemical removal mechanisms (Section 4.1.1). $^{224}\text{Ra}/^{228}\text{Ra}$ ratios exhibited no significant correlations with geochemical parameters in this study. Overall, $^5\text{Ra}/^4\text{Ra}$ in the investigated groundwater does not exhibit the elevated non-steady-state values expected during rapid mixing and salinization.

4.3.2. Estimating the alpha recoil flux

As discussed in Section 4.1.1, Ra levels in groundwater reflect a balance between source dominated by alpha recoil and chemical removal mechanisms. The supply of isotopes can be estimated by the activity of ^{222}Rn , the daughter of ^{226}Ra , because ^{222}Rn is inert and reaches higher activity in groundwater than ^{226}Ra . Therefore, variations in $^{222}\text{Rn}/^{226}\text{Ra}$ can be related to variations in the k_1/k_2 ratio (Krishnaswami et al., 1982, 1991). Radon-222 activities from the Cape Fear aquifer are generally low (median 2.9 Bq/L, range 2.9–52.1; Table 2). The resulting values of the $^{222}\text{Rn}/^{226}\text{Ra}$ activity ratio in the Cape Fear aquifer (median 541, range 73–4900) are also consistent with values expected in fresh to brackish sandstone aquifers (e.g. Krishnaswami et al., 1982; Szabo et al., 1997, 2005;

Tricca et al., 2001; Reynolds et al., 2003; Swarzenski et al., 2013). Similarly, Watson and Mitsch (1987) documented a range of low ^{222}Rn activities in Yorktown aquifer wells in eastern North Carolina (3–57 Bq/L) and reported a mean of 17 Bq/L. These low activities are consistent with the solid-phase radioactivity and groundwater Rn reported elsewhere in the Atlantic Coastal Plain aquifers (e.g. Szabo et al., 1997, 2005). Coastal plain sediments may contain elevated U-series radionuclides in phosphate deposits (Miller and Sutcliffe, 1985), which have been noted locally in the lower Yorktown formation (Section 1.2). However, there is no indication that high-phosphate deposits significantly affected Ra in the wells sampled during this study. Similar information on ^{222}Rn activities or solid-phase radionuclides is not available for the Morocco coastal aquifer, so significant variations in solid-phase radioactivity could occur within the aquifer solids, and if so, would be expected to influence observed groundwater radium levels.

4.3.3. Assessment of Ra removal mechanisms

4.3.3.1. Divalent vs. monovalent cation dominance: Implications for Ra adsorption or exchange.

Source and removal mechanisms for alkaline earth metals affect radium because the cation exchange environment in which Ca, Mg, and Sr are released is unfavorable for Ra removal and results in higher groundwater Ra than in monovalent-dominated waters (e.g. Nathwani and Phillips, 1979; Szabo et al., 2012; Swarzenski et al., 2013). The distinct cation composition between the two aquifer systems, in which MCA waters are enriched in divalent cations, can be seen in cation ratios (e.g. Ca/Na) and Cl-normalized cation concentrations (Fig. 2). The shallowest waters in the ACP (Section 3.2.1) exhibit higher Ra than would be expected for their TDS, chloride, or sulfate concentrations (Fig. 2g and h, Fig. 5), which could indicate that processes removing divalent cations overall have a specific role in removing Ra from ACP waters. Within the ACP aquifers, it seems that the shallow, low-TDS waters, and the deepest high-Cl brackish waters exhibit higher Ra than the Na– HCO_3^- waters of intermediate depth and distance along flowpaths.

4.3.3.2. Redox effects on Ra adsorption.

Although radium is not redox-sensitive, Mn and Fe oxides responsible for Ra adsorption are sensitive to reductive dissolution linked to microbial organic carbon oxidation in groundwater systems. Therefore, the presence of dissolved oxygen or nitrate provides thermodynamically stable conditions for solid-phase metal oxides that remove Ra from groundwater. Additionally, seawater intrusion may induce sulfate-reducing conditions by contributing high-sulfate water to organic-rich carbon coastal sediments (Section 4.1.2). In MCA, there seems to be no sulfate reduction induced by seawater intrusion because (1) dissolved oxygen was typically detectable in these waters (Table 1); (2) $\delta^{34}\text{S}-\text{SO}_4^{2-}$ never exceeds the modern seawater value of 21‰; (3) $\delta^{18}\text{O}-\text{SO}_4^{2-}$ does not exceed the modern seawater value of 9.5‰; and (4) values of $\delta^{34}\text{S}-\text{SO}_4^{2-}$ and $\delta^{18}\text{O}-\text{SO}_4^{2-}$ do not lie along a slope of 0.25 (Fig. 6; Table 2) as expected for sulfate reduction (Krouse and Mayer, 1999; Tuttle et al., 2009). Therefore, variations in $\delta^{34}\text{S}-\text{SO}_4^{2-}$ in MCA are consistent with mixing of sulfate sources (possibly including seawater, Atlas Mountains evaporites, and/or oxidized biogenic sulfide; Fig. 7), rather than sulfate reduction. In the Atlantic Coastal Plain aquifers, evidence for sulfate-reducing conditions includes low to non-detectable dissolved oxygen concentrations (Table 1) and highly positive values of $\delta^{34}\text{S}-\text{SO}_4^{2-}$ and $\delta^{18}\text{O}-\text{SO}_4^{2-}$ along the expected slope of 0.25 for sulfate reduction (Fig. 6). Overall in the ACP system, these sulfate-reducing conditions are unfavorable for abundant Ra adsorption sites to be present on highly reactive Mn and Fe oxides. However, it cannot be said that these metal oxides are absent, as Fe and Mn oxides have been observed in anoxic Atlantic Coastal Plain aquifer sediments, primarily in forms of low reactive surface area

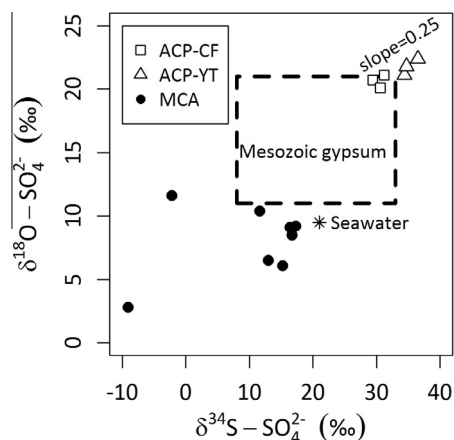


Fig. 6. $\delta^{34}\text{S}-\text{SO}_4^{2-}$ plotted against $\delta^{18}\text{O}-\text{SO}_4^{2-}$. Note that trends in ACP are consistent with sulfate reduction, whereas MCA data are mostly consistent with mixing and oxidation of sulfur sources.

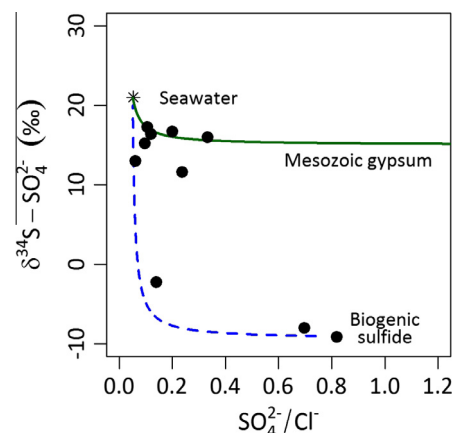


Fig. 7. Mixing of sulfate sources in MCA inferred from $\delta^{34}\text{S}-\text{SO}_4^{2-}$ and the $\text{SO}_4^{2-}/\text{Cl}^-$ ratio. “Mesozoic gypsum” represents the range of $\delta^{34}\text{S}-\text{SO}_4^{2-}$ and $\delta^{18}\text{O}-\text{SO}_4^{2-}$ in Mesozoic marine sulfate minerals (Claypool et al., 1980; Strauss, 1997). Solid green line represents mixing of seawater with Mesozoic marine gypsum of the Atlas Mountains (a hypothetical water with $\text{SO}_4^{2-}/\text{Cl}^-$ of 15, such as High Atlas spring AC-1 of Bouchaou et al. (2008), and with inferred $\delta^{34}\text{S}-\text{SO}_4^{2-} \approx 15\text{‰}$). Dashed blue line represents mixing of seawater with fresh water containing oxidized biogenic sulfide (a water like sample M9-47 with 500 mg/L SO_4^{2-} , $\delta^{34}\text{S}-\text{SO}_4^{2-} = -9\text{‰}$, and 250 mg/L Cl^-). (For interpretation of the references to colour in this figure legend, the reader is referred to the web version of this article.)

(Haque et al., 2008). In contrast to adsorption onto redox-sensitive Fe and Mn oxides, Ra removal onto the abundant clays in the ACP aquifers is not expected to be strongly affected by redox conditions.

4.3.3.3. Coprecipitation in barite.

In addition to its role as an alkaline earth metal in competing with Ra for adsorption or exchange sites, barium warrants detailed discussion because barite (BaSO_4) forms as a solid solution between Ba^{2+} and other divalent cations including trace Ra^{2+} . Whether high sulfate concentrations can facilitate radium removal in high-sulfate waters depends on whether barite saturation is reached and precipitation actually occurs, whereas the presence of high sulfate concentrations alone may enhance Ra solubility through formation of the uncharged RaSO_4^0 complex (Langmuir and Riese, 1985). In aquifers with active barite precipitation, Ba and SO_4^{2-} concentrations may be negatively correlated (e.g. Underwood et al., 2009). In MCA, the precipitation of barite

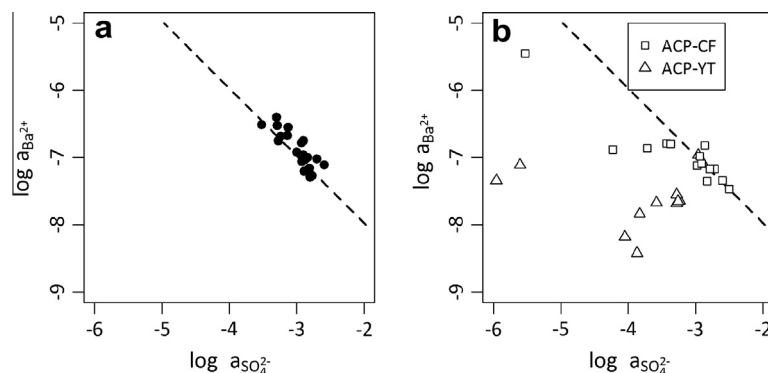


Fig. 8. Barium and sulfate ion activities for the Morocco coastal aquifer (a) and Atlantic Coastal Plain (b) aquifer systems in relationship to barite saturation at 25 °C (dashed line; $K_{sp} = 10^{-9.97}$; Drever, 1997).

may be a significant removal mechanism for Ra, indicated by (1) the negative correlation between Ba^{2+} and SO_4^{2-} ion activities consistently near barite saturation (median barite saturation index 0.10, range -0.12 to 0.35 ; Fig. 8a); (2) the negative correlation between Ra^{2+} and SO_4^{2-} ion activities, similar to the behavior of Ba^{2+} ($\rho = -0.60$); and (3) the apparent lack of sulfate-reducing conditions (Section 4.3.3.2). Here as with other sulfate-dominated waters (Section 4.1.1), the negative association between ^{226}Ra and SO_4^{2-} could imply that the presence of Ba is linked to Ra removal through coprecipitation. In contrast, if Ra removal were dominated by adsorption, higher sulfate might be associated with less efficient Ra removal and higher Ra. These results do not indicate that charge-sensitive removal (e.g. adsorption) is insignificant as a Ra removal mechanism in MCA; indeed the generally oxic conditions of the aquifer are consistent with effective adsorption to Mn and Fe oxides on the aquifer solids. The competitive relationship between coprecipitation and charge-sensitive removal (cation exchange or adsorption) depends on the availability of sites (e.g. Shao et al., 2009) and the relative rates of removal processes, which were not constrained by the methods utilized in this study.

In the ACP aquifers also, some high-sulfate waters reach barite saturation. A majority of Cape Fear aquifer waters are near barite saturation (median saturation index -0.02), but fewer Yorktown waters are (median saturation index -1.05 ; Fig. 8b). Despite the Cape Fear aquifer's apparent saturation with respect to barite, the Cape Fear aquifer exhibits no correlation between Ba concentration and Ra activities (Section 4.2), perhaps implying that removal mechanisms are not identical between Ba and Ra. The correlation noted by Szabo et al. (2012) in bicarbonate-dominated waters, of ^{226}Ra being positively associated with sulfate concentration (Section 4.1.1), was seen in the ACP aquifers, especially in the Yorktown aquifer ($\rho = 0.81$) but to some degree also in the Cape Fear aquifer ($\rho = 0.34$), essentially implying that $BaSO_4$ coprecipitation is not the main mechanism of Ra removal in the Yorktown and perhaps also in the Cape Fear. Overall, unlike MCA exhibiting reasonable evidence for Ba–Ra removal through secondary barite precipitation, the Yorktown aquifer is generally undersaturated with respect to barite. The potential importance of barite coprecipitation in the Cape Fear aquifer is ambiguous. Finally, it should be noted that the sulfate-reducing conditions in the ACP aquifer system (Section 4.3.3.2) are potentially unfavorable for the stable formation of barite (Section 4.1.1). It appears that charge-sensitive removal (adsorption and/or cation exchange) is dominant in the Yorktown aquifer and perhaps also in the Cape Fear aquifer.

5. Conclusions

Most of the waters examined in this study exhibited too low a salinity range for radium mobilization to be described by a linear

radium-salinity trend. Instead, the fresh to brackish waters lie within a transition zone between TDS-dependent and TDS-independent controls on Ra. TDS-independent controls include mechanisms that are driven by the presence of specific ions (e.g. competing divalent cations, barium, or sulfate) and/or by reducing conditions that cause redox-sensitive adsorption sites to be unstable (e.g. Mn and iron oxides). Therefore, detailed characterization of the nature and composition of salinity sources in aquifers undergoing salinization promotes improved understanding of how radium might be mobilized by changing environmental conditions. The observed levels of Ra in fresh to brackish groundwater exceed that expected from salinity-dependent desorption of Ra from solids, implying that salinity-independent radium source (α -recoil) and removal mechanisms are significant in the fresh to brackish waters.

Both the MCA and ACP aquifer systems seem to exhibit at least one effective radium removal process partially mitigating groundwater radium levels. These processes depend on local aquifer solids and geochemical conditions. We therefore suggest that a multi-tracer approach combining ion ratios, $^{87}Sr/^{86}Sr$, and sulfur and oxygen isotopes of sulfate provides insights on the complex and possibly overlapping mechanisms affecting radium occurrence and mobilization in aquifer systems. Fresh groundwater can, under some conditions, exhibit similar Ra activities as brackish groundwater in the same aquifer. However, it should be noted that Ra levels in the fresh (potable) to brackish groundwater investigated here are generally low relative to United States and international drinking water standards. Although groundwater chemistry, examined here, demonstrates mechanisms of effective Ra removal, aquifer solids were not available for analysis, and low levels of solid-phase radioactivity could influence the generally low levels of Ra observed in the studied groundwater.

In the Morocco coastal aquifer, the apparently oxic conditions are favorable for radium adsorption to the aquifer solids, but the abundance of other divalent cations in groundwater implies that there may be significant competition for adsorption or exchange sites. In addition, barite saturation and the negative correlation between ^{226}Ra and SO_4^{2-} imply that barite coprecipitation may be a significant radium removal mechanism. Although the competition between charge-sensitive Ra removal (adsorption/cation exchange) and removal through $BaSO_4$ precipitation was not specifically evaluated through the methods of this study, the relationship of sulfate with ^{226}Ra is consistent with barite having some role in removing radium, rather than radium being removed solely by the uptake of Ra^{2+} to adsorption or exchange sites. Therefore, although increasing salinity is generally associated with higher radium in groundwater, sulfate may impart significant radium-removing effects in waters in which barium is present. The findings of this study may not be uniformly applicable to cases of seawater

intrusion into coastal aquifers because geochemical tracers indicate seawater intrusion is only one of multiple possible salinity sources in the Morocco coastal aquifer. Broadly, these results illustrate the complex issues encountered in assessing an aquifer's response to salinization under generally oxic conditions.

In the anoxic Atlantic Coastal Plain system at near-neutral pH, the more saline samples exhibit an association between TDS concentrations and Ra content. However, complicating processes, especially at lower salinity, depend on the anion or cation composition of waters rather than simply TDS concentrations. The shallowest, lower-salinity waters are less dominated by Na than the deeper waters, and these shallow waters also exhibit higher Ra than would be expected from TDS concentrations alone. Essentially, these results imply that charge-sensitive adsorption and/or cation exchange are less effective at removing Ra from these shallow waters than elsewhere in the aquifer where cation exchange has yielded a more Na-dominant composition. In addition to charge-sensitive processes affecting Ra, barite precipitation is a possible but unresolved Ra removal mechanism in the Cape Fear aquifer. Overall, these results are consistent with Ra response to salinity and redox fluctuations in coastal sediments in which Ra levels are dependent on site-specific factors and not simply on TDS concentration (e.g. Gonneea et al., 2008). In the data presented in this study and other published investigations, Ra activity exhibits a more consistent linear increase with salinity above a threshold range of approximately 3000–10,000 mg/L TDS (Fig. 5b and c). In lower-salinity waters, that is, during the early phases of salinization, characterizing locally-variable Ra removal mechanisms could be especially important for the understanding of Ra response to salinity increases.

Acknowledgements

This study was supported by a NATO Science for Peace project (ESP.MD.SFPP 983134). We thank the Hydraulic Agency of Souss-Massa basin for their help throughout the project. Additional support was provided by the Nicholas School of the Environment at Duke University. Isotope analyses of sulfate were supported by a student research grant from the International Association of Geochemistry with the collaboration of B. Mayer and S. Taylor (University of Calgary). Additional field and laboratory assistance was provided by S. Boutaleb, Z. Lgourna, N. Ettayfi (Université Ibn Zohr); B. Peck, M. Gamble, N. Wilson, and staff of North Carolina Division of Water Resources; K. Flatt and staff of Dare County Water Department; and P. Heine, E. Klein, H. Schwartz, H. Raanan, and A. Zaino (Duke University). Finally, we thank Michael Kersten, Executive Editor of *Applied Geochemistry*, and the reviewers for their constructive comments.

References

- Ames, L.L., McGarrath, J.E., Walker, B.A., 1983a. Sorption of trace constituents from aqueous solutions onto secondary minerals. II. Radium. *Clays Clay Miner.* 31, 335–342.
- Ames, L.L., McGarrath, J.E., Walker, B.A., Salter, P.F., 1983b. Uranium and radium sorption on amorphous ferric oxyhydroxide. *Chem. Geol.* 40, 135–148.
- Andersen, M.S., Nyvang, V., Jakobsen, R., Postma, D., 2005. Geochemical processes and solute transport at the seawater/freshwater interface of a sandy aquifer. *Geochim. Cosmochim. Acta* 69, 3979–3994.
- Appelo, C.A.J., Postma, D., 1993. *Geochemistry, Groundwater, and Pollution*. Balkema, Rotterdam.
- Barlow, P.M., Reichard, E.G., 2010. Saltwater intrusion in coastal regions of North America. *Hydrogeol. J.* 18, 247–260.
- Ben Hamouda, M.F., Tarhouni, J., Leduc, C., Zouari, K., 2011. Understanding the origin of salinization of the Plio-quaternary eastern coastal aquifer of Cap Bon (Tunisia) using geochemical and isotope investigations. *Environ. Earth Sci.* 63, 889–901.
- Bolton, D.W., 2000. Occurrence and Distribution of Radium, Gross Alpha-Particle Activity, and Gross-Beta Particle Activity in Ground Water in the Magohy Formation and Potomac Group Aquifers, Upper Chesapeake Bay Area, Maryland. Maryland Geological Survey Report of Investigations 70.
- Bouchaou, L., Michelot, J.L., Vengosh, A., Hsissou, Y., Qurtobi, M., Gaye, C.B., Bullen, T.D., Zuppi, G.M., 2008. Application of multiple isotopic and geochemical tracers for investigation of recharge, salinization, and residence time of water in the Souss-Massa aquifer, southwest of Morocco. *J. Hydrol.* 352, 267–287.
- Brown, P.M., 1959. *Geology and Ground-Water Resources in the Greenville Area, North Carolina*. North Carolina Department of Conservation and Development, Bulletin 73.
- Chapelle, F.H., Knobel, L.L., 1983. Aqueous geochemistry and the exchangeable cation composition of glauconite in the Aquia Aquifer, Maryland. *Ground Water* 21, 343–352.
- Chapelle, F.H., Knobel, L.L., 1985. Stable carbon isotopes of HCO₃ in the Aquia Aquifer, Maryland; evidence for an isotopically heavy source of CO₂. *Ground Water* 23, 592–599.
- Chapelle, F.H., Zelibor, J.L., Grimes, D.J., Knobel, L.L., 1987. Bacteria in deep coastal plain sediments of Maryland: a possible source of CO₂ to groundwater. *Water Resour. Res.* 23, 1625–1632.
- Clark, I.D., Fritz, P., 1997. *Environmental Isotopes in Hydrogeology*. Lewis Publishers, Boca Raton, FL.
- Claypool, G.E., Holser, W.T., Kaplan, I.R., Sakai, H., Zak, I., 1980. The age curves of sulfur and oxygen isotopes in marine sulfate and their mutual interpretation. *Chem. Geol.* 28, 199–260.
- de Montety, V., Radakovich, O., Vallet-Coulomb, C., Blavoux, B., Hermitte, D., Valles, V., 2008. Origin of groundwater salinity and hydrogeochemical processes in a confined coastal aquifer: case of the Rhône delta (Southern France). *Appl. Geochem.* 23, 2337–2349.
- Denison, R.E., Hetherington, E.A., Bishop, B.A., Dahl, D.A., Koepnick, R.B., 1993. The use of strontium isotopes in stratigraphic studies: an example from North Carolina. *Southeastern Geol.* 33, 53–69.
- dePaul, V.T., Rice, D.E., Zapeca, O.S., 2008. Water-Level Changes in Aquifers of the Atlantic Coastal Plain, Predevelopment to 2000. US Geological Survey Scientific Investigations Report 2007-5247.
- Dickson, B.L., 1990. Radium in groundwater. In: *The Environmental Behaviour of Radium*, vol. 1. International Atomic Energy Agency, Technical Reports Series, 310, pp. 335–372.
- Dijon, R., 1969. Etude hydrogéologique et inventaire des ressources en eau de la vallée du Souss. *Notes et Mémoires du Service Géologique* 214.
- Drever, J.I., 1997. *The Geochemistry of Natural Waters: Surface and Groundwater Environments*, third ed. Prentice Hall, Upper Saddle River, NJ.
- Eaton, A.D., Clesceri, L.S., Rice, E.W., Greenberg, A.E. (Eds.), 2005. *Standard Methods for the Examination of Water and Wastewater*, 21st ed. American Public Health Association, Washington, DC.
- Fakir, Y., El Mernissi, M., Kreuser, T., Berjami, B., 2002. Natural tracer approach to characterize groundwater in the coastal Sahel of Oualidia (Morocco). *Environ. Geol.* 43, 197–202.
- García-Solsona, E., García-Orellana, J., Masqué, P., Dulaiova, H., 2008. Uncertainties associated with ²²³Ra and ²²⁴Ra measurements in water via a Delayed Coincidence Counter (RaDeCC). *Mar. Chem.* 109, 198–219.
- Gohn, G.S., 1988. Late Mesozoic and early Cenozoic geology of the Atlantic Coastal Plain: North Carolina to Florida. In: Sheridan, R.E., Grow, J.A. (Eds.), *The Atlantic Continental Margin: The Geology of North America*. Geological Society of America, Boulder, CO, pp. 67–85.
- Gonneea, M.E., Morris, P.J., Dulaiova, H., Charette, M.A., 2008. New perspectives on radium behavior within a subtropical estuary. *Mar. Chem.* 109, 250–267.
- Haluszczak, L.O., Rose, A.W., Kump, L.R., 2013. Geochemical evaluation of flowback brine from Marcellus gas wells in Pennsylvania, USA. *Appl. Geochem.* 28, 55–61.
- Haque, S., Ji, J., Johannesson, K.H., 2008. Evaluating mobilization and transport of arsenic in sediments and groundwaters of Aquia aquifer, Maryland, USA. *J. Contam. Hydrol.* 99, 68–84.
- Herczeg, A.L., Simpson, H.J., Anderson, R.F., Trier, R.M., Mathieu, G.G., Deck, B.L., 1988. Uranium and radium mobility in groundwaters and brines within the Delaware Basin, Southeastern New Mexico, USA. *Chem. Geol.* 72, 181–196.
- Hsissou, Y., Bouchaou, L., Mudry, J., Mania, J., Chauve, P., 2002. Use of chemical tracing to study acquisition modalities of the mineralization and behaviour of unconfined groundwaters under a semi-arid climate; the case of the Souss Plain (Morocco). *Environ. Geol.* 42, 672–680.
- Jones, B.F., Vengosh, A., Rosenthal, E., Yechieli, Y., 1999. Geochemical investigations. In: Bear, J., Cheng, A.H.-D., Sorek, S., Ouazar, D., Herrera, I. (Eds.), *Seawater Intrusion in Coastal Aquifers – Concepts, Methods, and Practices*. Kluwer Academic Publishers, Dordrecht, Netherlands, pp. 51–71.
- Katz, B.G., Bullen, T.D., 1996. The combined use of ⁸⁷Sr/⁸⁶Sr and carbon and water isotopes to study the hydrochemical interaction between groundwater and lakewater in mantled karst. *Geochim. Cosmochim. Acta* 60, 5075–5087.
- Kennedy, C.D., Genereux, D.P., 2007. ¹⁴C groundwater age and the importance of chemical fluxes across aquifer boundaries in confined Cretaceous aquifers of North Carolina, USA. *Radiocarbon* 49, 1181–1203.
- Khaska, M., Salle, C.L.G.L., Lancelot, J., ASTER team, Mohamad, A., Verdoux, P., Noret, A., Simler, R., 2013. Origin of groundwater salinity (current seawater vs. saline deep water) in a coastal karst aquifer based on Sr and Cl isotopes. Case study of the La Clape massif (southern France). *Appl. Geochem.* (in press). <http://dx.doi.org/10.1016/j.apgeochem.2013.07.006>.
- Kim, G., Burnett, W.C., Dulaiova, H., Swarzenski, P.W., Moore, W.S., 2001. Measurement of ²²⁴Ra and ²²⁶Ra activities in natural waters using a radon-in-air monitor. *Environ. Sci. Technol.* 35, 4680–4683.

- Knobel, L.L., Chapelle, F.H., Meisler, H., 1998. Geochemistry of the Northern Atlantic Coastal Plain Aquifer System. US Geological Survey Professional Paper 1404-L.
- Kraemer, T.F., Reid, D.F., 1984. The occurrence and behavior of radium in saline formation water of the U.S. Gulf Coast region. *Isot. Geosci.* 2, 153–174.
- Krest, J.M., Moore, W.S., Rama, 1999. ^{226}Ra and ^{228}Ra in the mixing zones of the Mississippi and Atchafalaya Rivers: indicators of groundwater input. *Mar. Chem.* 64, 129–152.
- Krishnaswami, S., Bhushan, R., Baskaran, M., 1991. Radium isotopes and ^{222}Rn in shallow brines, Kharaghoda (India). *Chem. Geol. Isot. Geosci. Sect.* 87, 125–136.
- Krishnaswami, S., Graustein, W.C., Turekian, K.K., Dowd, J.F., 1982. Radium, thorium, and radioactive lead isotopes in groundwaters: application to the in situ determination of adsorption–desorption rate constants and retardation factors. *Water Resour. Res.* 18, 1663–1675.
- Krouse, H.R., Mayer, B., 1999. Sulphur and oxygen isotopes in sulphate. In: Cook, P., Herczeg, A.L. (Eds.), *Environmental Tracers in Subsurface Hydrology*. Kluwer Academic Publishers, Dordrecht, Netherlands, pp. 195–232.
- Lamontagne, S., Le Gal La Salle, C., Hancock, G.J., Webster, I.T., Simmons, C.T., Love, A.J., James-Smith, J., Smith, A.J., Kämpf, J., Fallowfield, H.J., 2008. Radium and radon radioisotopes in regional groundwater, intertidal groundwater, and seawater in the Adelaide Coastal Waters Study area: implications for the evaluation of submarine groundwater discharge. *Mar. Chem.* 109, 318–336.
- Langmuir, D., Riese, A.C., 1985. The thermodynamic properties of radium. *Geochim. Cosmochim. Acta* 49, 1593–1601.
- Li, Y.-H., Chan, L.-H., 1979. Desorption of Ba and ^{226}Ra from river-borne sediments in the Hudson estuary. *Earth Planet. Sci. Lett.* 43, 343–350.
- Martin, A.J., Crusius, J., McNeel, J.J., Yanful, E.K., 2003. The mobility of radium-226 and trace metals in pre-oxidized subaqueous uranium mill tailings. *Appl. Geochem.* 18, 1095–1110.
- McArthur, J.M., Howarth, R.J., Bailey, T.R., 2001. Strontium isotope stratigraphy; LOWESS Version 3; best fit to the marine Sr-isotope curve for 0–509 Ma and accompanying look-up table for deriving numerical age. *J. Geol.* 109, 155–170.
- McMahon, P.B., Chapelle, F.H., 1991. Microbial production of organic acids in aquitard sediments and its role in aquifer geochemistry. *Nature* 349, 233–235.
- Meisler, H., 1989. The Occurrence and Geochemistry of Salty Ground Water in the Northern Atlantic Coastal Plain. US Geological Survey Professional Paper 1404-D.
- Michael, H.A., Charette, M.A., Harvey, C.F., 2011. Patterns and variability of groundwater flow and radium activity at the coast: a case study from Waquoit Bay, Massachusetts. *Mar. Chem.* 127, 100–114.
- Miller, R.L., Sutcliffe, H., 1985. Occurrence of Natural Radium-226 Radioactivity in Ground Water of Sarasota County, Florida. US Geological Survey Water-Resources Investigations Report 84-8237.
- Millero, F.J., Sohn, M.L., 1991. *Chemical Oceanography*. CRC Press, Boca Raton, FL.
- Moise, T., Starinsky, A., Katz, A., Kolodny, Y., 2000. Ra isotopes and Rn in brines and ground waters of the Jordan-Dead Sea Rift Valley: enrichment, retardation, and mixing. *Geochim. Cosmochim. Acta* 64, 2371–2388.
- Moore, W.S., Arnold, R., 1996. Measurement of ^{223}Ra and ^{224}Ra in coastal waters using a delayed coincidence counter. *J. Geophys. Res.* 101, 1321–1329.
- Moore, W.S., Reid, D.F., 1973. Extraction of radium from natural water using manganese impregnated acrylic fibers. *J. Geophys. Res.* 78, 8880–8886.
- Nadler, A., Magaritz, M., Mazar, E., 1980. Chemical reactions of sea water with rocks and freshwater: experimental and field observations on brackish waters in Israel. *Geochim. Cosmochim. Acta* 44, 879–886.
- Nathwani, J.S., Phillips, C.R., 1979. Adsorption of ^{226}Ra by soils in the presence of Ca^{2+} ions. Specific adsorption (II). *Chemosphere* 8, 293–299.
- Otero, N., Soler, A., Corp, R.M., Mas-Pla, J., Garcia-Solsona, E., Masqué, P., 2011. Origin and evolution of groundwater collected by a desalination plant (Tordera, Spain): a multi-isotopic approach. *J. Hydrol.* 397, 37–46.
- Ouda, B., El Hamdaoui, A., Ibn Majah, M., 2005. Isotopic composition of precipitation at three Moroccan stations influenced by oceanic and Mediterranean air masses. In: *Isotopic Composition of Precipitation in the Mediterranean Basin in Relation to Air Circulation Patterns and Climate: Final Report of a Coordinated Research Project 2000–2004*. International Atomic Energy Agency IAEA-TECDOC-1453, pp. 125–140.
- Parkhurst, D.L., Appelo, C.A.J., 1999. User's Guide to PHREEQC (Version 2) – A Computer Program for Speciation, Batch-Reaction, One-Dimensional Transport, and Inverse Geochemical Calculations. US Geological Survey Water-Resources Investigations Report 99-4259.
- R Core Team, 2013. R: A Language and Environment for Statistical Computing (Software Version 3.0.1). <<http://www.R-project.org>>.
- Reynolds, B.C., Wasserburg, G.J., Baskaran, M., 2003. The transport of U- and Th-series nuclides in sandy confined aquifers. *Geochim. Cosmochim. Acta* 67, 1955–1972.
- Riggs, S.R., Belknap, D.F., 1988. Upper Cenozoic processes and environments of continental margin sedimentation: Eastern United States. In: Sheridan, R.E., Grow, J.A. (Eds.), *The Atlantic Continental Margin: The Geology of North America*. Geological Society of America, Boulder, CO, pp. 131–176.
- Rowan, E.L., Engle, M.A., Kirby, C.S., Kraemer, T.F., 2011. Radium Content of Oil- and Gas-Field Produced Waters in the Northern Appalachian Basin (USA): Summary and Discussion of Data. US Geological Survey Scientific Investigations Report 2011-5135.
- Russak, A., Sivan, O., 2010. Hydrogeochemical tool to identify salinization or freshening of coastal aquifers determined from combined field work, experiments, and modeling. *Environ. Sci. Technol.* 44, 4096–4102.
- Shao, H., Kulik, D.A., Kosakowski, G., Kolditz, O., 2009. Modeling the competition between solid solution formation and cation exchange on the retardation of aqueous radium in an idealized bentonite column. *Geochem. J.* 43, e37–e42.
- Sivan, O., Yechieli, Y., Herut, B., Lazar, B., 2005. Geochemical evolution and timescale of seawater intrusion into the coastal aquifer of Israel. *Geochim. Cosmochim. Acta* 69, 579–592.
- Sposito, G., 2008. *The Chemistry of Soils*, second ed. Oxford University Press, Oxford.
- Strauss, H., 1997. The isotopic composition of sedimentary sulfur through time. *Palaogeogr. Palaeoclimatol.* 132, 97–118.
- Sturchio, N.C., Banner, J.L., Binz, C.M., Heraty, L.B., Musgrove, M., 2001. Radium geochemistry of ground waters in Paleozoic carbonate aquifers, midcontinent, USA. *Appl. Geochem.* 16, 109–122.
- Swarzenski, P.W., Baskaran, M., Rosenbauer, R.J., Edwards, B.D., Land, M., 2013. A combined radio- and stable-isotopic study of a California coastal aquifer system. *Water* 5, 480–504.
- Szabo, Z., dePaul, V.T., Fischer, J.M., Kraemer, T.F., Jacobsen, E., 2012. Occurrence and geochemistry of radium in water from principal drinking-water aquifer systems of the United States. *Appl. Geochem.* 27, 729–752.
- Szabo, Z., dePaul, V.T., Kraemer, T.F., Parsa, B., 2005. Occurrence of Radium-224, Radium-226, and Radium-228 in Water of the Unconfined Kirkwood-Cohansey Aquifer System, Southern New Jersey. US Geological Survey Scientific Investigations Report 2004-5224.
- Szabo, Z., Rice, D.E., MacLeod, C.L., Barringer, T.H., 1997. Relation of Distribution of Radium, Nitrate, and Pesticides to Agricultural Land Use and Depth, Kirkwood-Cohansey Aquifer System, New Jersey Coastal Plain, 1990–1991. US Geological Survey Water-Resources Investigations Report 96-4165.
- Szabo, Z., Zapecka, O.S., 1987. Relation between natural radionuclide activities and chemical constituents in ground water in the Newark Basin, New Jersey. In: Graves, B. (Ed.), *Radon, Radium, and Other Radioactivity in Ground Water*. Lewis Publishers, Chelsea, MI, pp. 283–308.
- Tagma, T., 2005. Caractérisation de la minéralisation des eaux souterraines de la nappe côtière d'Agadir: répartition et origine. Master's thesis, Université Ibn Zohr, Agadir, Morocco.
- Tomita, J., Satake, H., Fukuyama, T., Sasaki, K., Sakaguchi, A., Yamamoto, M., 2010. Radium geochemistry in Na-Cl type groundwater in Niigata Prefecture, Japan. *J. Environ. Radioact.* 101, 201–210.
- Tricca, A., Wasserburg, G.J., Porcelli, D., Baskaran, M., 2001. The transport of U- and Th-series nuclides in a sandy unconfined aquifer. *Geochim. Cosmochim. Acta* 65, 1187–1210.
- Tuttle, M.L.W., Breit, G.N., Cozzarelli, I.M., 2009. Processes affecting $\delta^{34}\text{S}$ and $\delta^{18}\text{O}$ values of dissolved sulfate in alluvium along the Canadian River, central Oklahoma, USA. *Chem. Geol.* 265, 455–467.
- Underwood, E.C., Ferguson, G.A., Betcher, R., Phipps, G., 2009. Elevated Ba concentrations in a sandstone aquifer. *J. Hydrol.* 376, 126–131.
- Vengosh, A., in press. Salinization and saline environments. In: Sherwood Lollar, B. (Ed.), *Environmental Geochemistry. Treatise on Geochemistry*, vol. 9, second ed. Elsevier.
- Vengosh, A., Gill, J., Davisson, M.L., Hudson, G.B., 2002. A multi-isotope (B, Sr, O, H, and C) and age dating (^3H - ^3He and ^{14}C) study of groundwater from Salinas Valley, California: hydrochemistry, dynamics, and contamination processes. *Water Resour. Res.* 38. <http://dx.doi.org/10.1029/2001WR000517>.
- Vengosh, A., Hirschfeld, D., Vinson, D., Dwyer, G., Raanan, H., Rimawi, O., Al-Zoubi, A., Akkawi, E., Marie, A., Haquin, G., Zaarur, S., Ganor, J., 2009. High naturally occurring radioactivity in fossil groundwater from the Middle East. *Environ. Sci. Technol.* 43, 1769–1775.
- Vengosh, A., Kloppmann, W., Marei, A., Livshitz, Y., Gutierrez, A., Banna, M., Guerrot, C., Pankratov, I., Raanan, H., 2005. Sources of salinity and boron in the Gaza strip: natural contaminant flow in the southern Mediterranean coastal aquifer. *Water Resour. Res.* 41, 1–19.
- Vengosh, A., Spivack, A.J., Artzi, Y., Ayalon, A., 1999. Geochemical and boron, strontium, and oxygen isotopic constraints on the origin of the salinity in groundwater from the Mediterranean coast of Israel. *Water Resour. Res.* 35, 1877–1894.
- Vinson, D.S., Lundy, J.R., Dwyer, G.S., Vengosh, A., 2012. Implications of carbonate-like geochemical signatures in a sandstone aquifer: radium and strontium isotopes in the Cambrian Jordan aquifer (Minnesota, USA). *Chem. Geol.* 334, 280–294.
- Vinson, D.S., Schwartz, H.G., Dwyer, G.S., Vengosh, A., 2011. Evaluating salinity sources of groundwater and implications for sustainable reverse osmosis desalination in coastal North Carolina, USA. *Hydrogeol. J.* 19, 981–994.
- Warner, N.R., Jackson, R.B., Darrah, T.H., Osborn, S.G., Down, A., Zhao, K., White, A., Vengosh, A., 2012. Geochemical evidence for possible natural migration of Marcellus Formation brine to shallow aquifers in Pennsylvania. *Proc. Natl. Acad. Sci.* 109, 11961–11966.
- Watson, J.E., Mitsch, B.F., 1987. Ground-water concentrations of ^{226}Ra and ^{222}Rn in North Carolina phosphate lands. *Health Phys.* 52, 361–365.
- Webster, I.T., Hancock, G.J., Murray, A.S., 1995. Modelling the effect of salinity on radium desorption from sediments. *Geochim. Cosmochim. Acta* 59, 2469–2476.
- Winner, M.D., Coble, R.W., 1996. Hydrogeologic Framework of the North Carolina Coastal Plain. US Geological Survey Professional Paper 1404-I.
- Wood, W.W., Kraemer, T.F., Shapiro, A., 2004. Radon (^{222}Rn) in ground water of fractured rocks: a diffusion/ion exchange model. *Ground Water* 42, 552–567.
- Woods, T.L., Fullagar, P.D., Spruill, R.K., Sutton, L.C., 2000. Strontium isotopes and major elements as tracers of ground water evolution: example from the Upper Castle Hayne Aquifer of North Carolina. *Ground Water* 38, 762–771.
- Yamanaka, M., Kumagai, Y., 2006. Sulfur isotope constraint on the provenance of salinity in a confined aquifer system of the southwestern Nobi Plain, central Japan. *J. Hydrol.* 325, 35–55.
- Zielinski, R.A., Budahn, J.R., 2007. Mode of occurrence and environmental mobility of oil-field radioactive material at US Geological Survey research site B, Osage-Skiatook Project, northeastern Oklahoma. *Appl. Geochem.* 22, 2125–2137.